

- Line 32: It is not good to start a sentence with a symbol. I suggest to write: Emission of anthropogenic origin CO₂ ...

The suggestion has been included in the new version of the manuscript

- Line 49: IOC is a UNESCO body. To be more precise substitute United Nations with UNESCO

The suggestion has been included in the new version of the manuscript

- Line 326: following the suggestion of a referee, here I am recommending to change the sentence in: ... error was 0.003, using the equation of practical salinity given by UNESCO (1981) ...

The suggestion has been included in the new version of the manuscript

- Line 413: A quality flag ... Please, specify in parenthesis what QC flags convention are you using (SeaDataNet? WOCE? ...)

The quality control flags in the previous version was a mixture of WOCE bottle flagging and SEADATANET codes, since following a reviewer's recommendation we assigned a flag of "6" to values below the detection limit. As we are using WHP-Exchange bottle format for the database, we believe it would be best to use an unique convection, namely WOCE bottle. Therefore, we will assign a code of "2" to those values that were flagged as "6" according to the SEADATANET flags. We will make this change in the repository, as soon as we know your opinion on this issue. The new sentence is:

" A quality control flag value following the recommendations from WOCE bottle data flagging quality codes was assigned to each measurement available from the repository sites (Table 1)."

1 **ARIOS: a database for ocean acidification assessment in the Iberian Upwelling**
2 **System (1976 - 2018).**

3
4 **Xosé Antonio Padin*¹, Antón Velo¹ and Fiz F. Pérez¹**

5 ¹ Instituto de Investigaciones Marinas, IIM-CSIC, 36208 Vigo, Spain.

6 padin@iim.csic.es, avelo@iim.csic.es, fiz.perez@iim.csic.es

7
8 **1. Abstract**

9 A data product of 17,653 discrete samples from 3,343 oceanographic stations
10 combining measurements of pH, alkalinity and other biogeochemical parameters off the
11 North-western Iberian Peninsula from June 1976 to September 2018 is presented in this
12 study. The oceanography cruises funded by 24 projects were primarily carried out in the
13 *Ría de Vigo* coastal inlet, but also in an area ranging from the Bay of Biscay to the
14 Portuguese coast. The robust seasonal cycles and long-term trends were only calculated
15 along a longitudinal section, gathering data from the coastal and oceanic zone of the
16 Iberian Upwelling System. The pH in the surface waters of these separated regions,
17 which were highly variable due to intense photosynthesis and the remineralization of
18 organic matter, showed an interannual acidification ranging from -0.0016 yr^{-1} to -0.0039
19 yr^{-1} that grew towards the coastline. This result is obtained despite the buffering
20 capacity increasing in the coastal waters further inland as shown by the increase in
21 alkalinity by $1.1 \pm 0.7 \mu\text{mol kg}^{-1} \text{ yr}^{-1}$ and $2.6 \pm 1.0 \mu\text{mol kg}^{-1} \text{ yr}^{-1}$ in the inner and outer *Ría*
22 *de Vigo* respectively, driven by interannual changes in the surface salinity of
23 $0.0193 \pm 0.0056 \text{ psu yr}^{-1}$ and $0.0426 \pm 0.016 \text{ psu yr}^{-1}$ respectively. The loss of the vertical
24 salinity gradient in the long-term trend in the inner ría was consistent with other
25 significant biogeochemical changes such as a lower oxygen concentration and
26 fertilization of the surface waters. These findings seem to be related to a growing
27 footprint of sediment remineralization of organic matter in the surface layer of a more
28 homogeneous water column.

29 Data are available at: <http://dx.doi.org/10.20350/digitalCSIC/12498> (Pérez et al., 2020).

30

31 **2. Introduction**

32 Emissions of anthropogenic origin CO_2 (fossil fuels, land use and cement
33 manufacturing) into the atmosphere are the main cause behind the warming of the Earth
34 due to the greenhouse effect (IPCC, 2013). Given the constant exchange of gases
35 through the air-sea interface, the oceanic reservoir plays a key role as a sink for about

TONI PADIN 31/7/2020 15:05

Eliminado: CO_2 e

TONI PADIN 31/7/2020 15:05

Con formato: Subíndice

37 31% of anthropogenic CO₂ emissions (Sabine et al., 2004), controlling the partial
38 pressure of carbon dioxide in the atmosphere and regulating global temperatures.

39

40 The CO₂ uptake by the oceans produces changes in the inorganic carbon system in spite
41 of being partially dampened by the seawater buffering capacity. This ability of seawater
42 to withdraw anthropogenic CO₂ becomes more limited as more CO₂ is absorbed, which
43 will make it difficult to stabilize atmospheric CO₂ in the future (Orr et al., 2009). The
44 gradual absorption of atmospheric CO₂ by the oceans decreases seawater pH, causing
45 ocean acidification, which conditions the buffering capacity of seawater and in turn the
46 exchange of CO₂ between the ocean and the atmosphere (Caldeira and Wickett, 2003;
47 Raven et al., 2005). This effect of CO₂ absorption, which is known as ocean
48 acidification, conditions the buffering capacity of seawater and to some extent the
49 exchange of CO₂ between the ocean and the atmosphere. The Intergovernmental
50 Oceanographic Commission of the [UNESCO](#) identified the chemical change in
51 seawater brought about by ocean acidification as an indicator of a stressor on marine
52 ecosystems with a negative impact on socio-economic activities such as fishing and
53 shellfish farming. Hence, it was necessary for the oceanography community to observe
54 and gather data about pH and other parameters of the marine carbon system to conduct
55 accurate measurements of pH and ancillary parameters and provide data products to
56 help a sustainable management of the marine resources. The effect of ocean
57 acidification on marine ecosystems has stimulated impetus in the international
58 community for gathering high quality time-series measurements of the marine inorganic
59 carbon system (Hofmann et al., 2011; Andersson and MacKenzie, 2012; McElhany and
60 Busch, 2013; Takeshita et al., 2015; Wahl et al., 2016) and for predicting the future
61 evolution of the pH caused by climate change.

62

63 The threat for oceanic acidification of marine ecosystems is especially significant in
64 regions like coastal upwelling areas, which are more sensitive and appear to respond
65 faster to anthropogenic perturbations (Feely et al., 2008; Gruber et al., 2012; Lachkar,
66 2014; Hauri et al., 2013). These ecosystems are characteristic for their complex physical
67 and biogeochemical interactions and for sustaining enormous biological productivity
68 and productive fisheries (Pauly and Christensen, 1995; Hauri et al., 2009). The
69 photosynthetic activity in these regions is also an important mechanism for the seawater
70 CO₂ uptake, converting most of these areas into atmospheric CO₂ sinks (Pérez et al.,

TONI PADIN 31/7/2020 15:06

Eliminado: United Nations

72 1999; Cobo-Viveros et al., 2013). However, the high physical/chemical variability in
73 short temporal and spatial scales of upwelling systems and the lack of regular sampling
74 in these waters prevents a complete picture of the acidification of these ecosystems.

75

76 In the Iberian Upwelling System, the researchers of the Instituto de Investigaciones
77 Mariñas (IIM-CSIC) since 1976 commenced accurate measurements of marine
78 inorganic carbon system and associated parameters. As a result, a collection of pH
79 observations and ancillary biogeochemical information along the Galicia coast (40°N
80 and 45°N, 11°W) has been gathered under the framework of different projects over the
81 past 40 years. The current database, hereinafter called ARIOS (Acidification in the rias
82 and the Iberian continental shelf) database, holds biogeochemical information from
83 3,357 oceanographic stations, giving 17,653 discrete samples. This unique collection is
84 a starting point for evaluating the ocean acidification in the Iberian Upwelling System
85 characterized by intense biogeochemical interactions as an observation-based analysis,
86 or for use as inputs in a coupled physical-biogeochemical model to disentangle these
87 interactions at the ecosystem level.

88

89 **3. Data provenance**

90 **3.1. Data spatial coverage**

91 The main characteristic of the Galician coastline, located in the north-west of the
92 Iberian Peninsula, is the *Rías Baixas*, four long coastal estuaries or rias (>2.5 km³)
93 between 42°N and 43°N (Fig. 1). The water exchange between the *Rías Baixas* and open
94 waters is drastically affected by the coastal wind pattern as part of the Canary Current
95 Upwelling System (Wooster et al., 1976; Fraga 1981; Arístegui et al., 2004). Under the
96 predominance of northeasterly winds (Blanton et al., 1984) during spring-summer, the
97 surface offshore transport of surface waters leads to a rising cold, nutrient-rich, deep
98 water mass called the Eastern North Atlantic Central Water (ENACW) (Ríos et al.,
99 1992). Under these conditions, the *Rías Baixas* act as an extension of the continental
100 shelf (Rosón et al., 1995; Souto et al., 2003; Gilcoto et al., 2017), where upwelling
101 filaments extending westward export primary production from the coast into the ocean
102 (Álvarez-Salgado et al., 2001). In the opposite direction, the prevalence of northward
103 winds (Blanton et al., 1984) moves the surface waters towards the coast, where they
104 accumulate, sink and thus isolate the coast. This process, known as downwelling, is
105 typical during the autumn-winter along with other characteristics such as the warm,

106 salty waters from the Iberian Poleward Current (IPC) of subtropical origin (Fraga et al.,
107 1982; Alvarez-Salgado et al., 2006) that flows constrained to the Iberian shelf break
108 (Frouin et al., 1990). The run-off from local rivers also contributes to the presence of
109 river plumes over the shelf (Otero et al., 2008). These hydrodynamic conditions, the
110 meteorological forcings and the alternation of periods of upwelling and downwelling
111 (Álvarez, 1999; Gago et al., 2003c; Cobo-Viveros et al., 2013) stimulate the
112 development of intense primary production and high rates of recycling and downward
113 carbon export (Alonso-Pérez and Castro, 2014). The result of this biogeochemical
114 variability in terms of air-sea CO₂ exchange is that the surface waters act as a net CO₂
115 sink that is especially intense and variable over the shelf compared to offshore or in the
116 inner *Rías Baixas* (Padin et al., 2010).

117

118 Besides the short-term and seasonal variability, significant changes in the long-term
119 scale have been reported in this region. In addition to changes such as the weakening
120 and shortening of the upwelling events (Lemos and Sansó, 2006; Pérez et al., 2010;
121 Alvarez-Salgado et al., 2009), the warming (González-Pola et al., 2005; Pérez et al.,
122 2010) and changes in the composition of phytoplankton (Bode et al., 2009; Pérez et al.,
123 2010), the acidification in the first 700 metres for the geographical area from the Iberian
124 Peninsula to the 20° W meridian and from 36°N to 43°N has also been observed at a rate
125 of -0.0164 pH units per decade (Ríos et al., 2001; Castro et al. 2009).

126

127 **3.2. Distribution of sampling**

128 According to the type of region under study, different areas were identified in order to
129 classify the measurements gathered in the oceanographic cruises (Fig. 1). The latitude
130 of 43°N where Cape Finisterre is located was used as the dividing line between northern
131 and southern waters. Subsequently, a criterion of depth also split the waters to the north
132 of 43°N into north oceanic (below 250 m), north shelf (between 205 m and 75 m) and
133 north coast (75 m to the surface). The southern shelf waters were divided by latitude
134 42°N into Portuguese and the *Rías Baixas* (RB) shelves, whereas the shallower waters
135 were identified by the main rias, where three different zones were defined using
136 longitude boundaries (outer, middle and inner) according to Gago et al. (2003c) in the
137 *Ría de Vigo*, and just two zones in the other rias (*Ría de Pontevedra*, *Ría de Arousa*, *Ría*
138 *de Muros*). Southern waters between the isobath at 75 metres and the mouth of the
139 estuaries were identified as the Portuguese and RB coast.

140

141 The discrete measurements gathered in the ARIOS dataset were mainly found in
142 different regions' waters around 42°N latitude (Fig 1; Fig. 2a), especially in the outer
143 and middle areas of the *Ría de Vigo*, which accounted for 15% and 21% of the total
144 measurements respectively due to the proximity to the *Instituto de Investigaciones*
145 *Mariñas* (IIM-CSIC). Most of the measurements (85%) carried out by many of these
146 cruises to study the coastal ecosystems concentrated on shallow waters between the
147 seawater surface and 75 metres in depth (Fig. 2b). Although waters below 4,900 metres
148 deep were also sampled, observations below 900 metres only account for 1% of the
149 ARIOS database.

150

151 The observations made over more than 40 years in every region of the ARIOS database
152 were irregular on both an interannual and seasonal scale (Fig. 2a). The period of most
153 sampling activity was the 80s and 90s, whereas samples were especially scarce in the
154 early 2010s. On a seasonal scale, summer and autumn were the preferred seasons to
155 address the different research purposes, with 37% and 36% of the total samples
156 respectively. The observations taken during less favourable winter conditions,
157 especially aboard the coastal vessels usually available, only accounted for the 10% of
158 the ARIOS database.

159

160 **3.3. Data sources**

161 The ARIOS database is a compilation of biogeochemical properties with discrete
162 measurements of temperature, salinity, oxygen, nutrients, alkalinity, pH and chlorophyll
163 that were sampled in waters off the northwest of the Iberian Peninsula from 1976 to
164 2018 and measured by IIM-CSIC (Table 1). This data collection is part of the research
165 by 24 projects and oceanographic cruises conducted in response to different aims. The
166 different sampling strategies built up an irregular biogeochemical database whose
167 particular frequency and spatial coverage is shown in Figure 2.

168

169 The contribution to the ARIOS database from the oceanographic cruises and projects
170 over the different decades is described below.

171

172 **Cruises in the 70s and 80s:**

173 The first three cruises were carried out over three periods (1976, 1981-1983 and 1983-
174 1984), sampling the *Ría de Vigo*. These cruises were designed to provide environmental
175 information (upwelling events, estuarine circulation, continental inputs, etc.) for
176 research into the biology of some fish species. They measured identical parameters in
177 the Vigo estuary but at different stations and frequency.

178

179 In the summer of 1984, the *Galicia VIII* cruise studied the summer upwelling events
180 occurring on the contact front between the two ENACW water masses off Cape
181 Finisterre from short sections perpendicular to the Galician coast with 85 stations
182 offshore and 35 stations over the shelf. This cruise marked a milestone in the
183 oceanographic research of IIM-CSIC because it was the first time that the parameters of
184 the carbon system were measured on-board in offshore waters. Moreover,
185 measurements of a particular station on the shelf break with a bottom depth of 600
186 metres were taken every two days for a month, including two-day continuous
187 samplings.

188

189 Two years later, the Ria de Vigo 1986 sampled along the main axis of the Ria de Vigo
190 in 7 monthly repetitions during the first half of the year in which the primary production
191 and the organic matter exchange between the estuary and the shelf was studied in
192 relation to the hydrographic regime. Shortly afterwards, the same topic was also
193 researched by the Galicia IX project in September and October 1986 from 145 stations,
194 50 of which were coastal and 80 located in ocean waters (Prego et al., 1990).

195

196 The following year, the 1987 Provigo project (Nogueira et al., 1997) initiated a periodic
197 study from a fixed site (42°14.5'N, 8°45.8'W) located in the main channel in the middle
198 zone of the *Ría de Vigo*. This oceanographic station was selected as suitable for
199 evaluating the main processes that occur in the inner ria associated with external forcing
200 changes (Rios, 1992; Figueiras et al., 1994). Although the Provigo project finished in
201 1996, the fixed station was repeatedly included in subsequent cruises, extending the
202 time series at this location until today, when it is currently sampled every week by
203 INTECMAR (www.intecmar.gal). An example of the subsequent sampling repetition of
204 this station occurred the following year when one of the three stations in the Vigo
205 estuary in the Luna 1988 project (Fraga et al., 1992) took a sample every two weeks to

206 study the environmental control over the phytoplankton populations throughout an
207 annual cycle (February 1988 - February 1989).

208

209 At the end of 80s, the carbon system monitoring by the IIM-CSIC was extended to the
210 *Ría de Arousa* throughout 1989 (Álvarez-Salgado et al., 1993; Perez et al., 2000) in
211 order to learn the effect of upwelling on the water circulation pattern, community
212 production and the fluxes and net budgets of biogenic constituents in this ria with the
213 highest mussel production in Europe. For 5 months, 11 stations' samples were repeated
214 twice a week in the ria that is the most productive, housing intense cultivation of
215 mussels on rafts (Blanton et al., 1984).

216

217 **Cruises of the 90s:**

218 In the first half of this decade, studying the phytoplankton communities was the
219 oceanographic cruises' most relevant aim, concentrating particularly on harmful algae
220 blooms. The hydrodynamic and biogeochemical conditions controlling the growth,
221 development and migration of the phytoplankton were analysed both in the interior of
222 the estuary and on the continental shelf.

223

224 For five days in September, the 1990 *Ría de Vigo* cruise (Figueiras et al., 1994) sampled
225 five stations distributed along the longitudinal axis of the ria and one at the northern
226 mouth. The next year, the cruise Galicia XI was carried out in May, sampling at 39
227 stations along eight transects perpendicular to the coastline; and Galicia XII (Alvarez-
228 Salgado et al., 1998, 2002, 2003; Castro et al., 1994) in September, sampling at 37
229 oceanic stations and 7 coastal stations.

230

231 The *Ría de Vigo* cruise in 1993-4 (Miguez et al., 2001), with four stations using 24
232 repetitions with a CTD-SBE25, investigated the hydrodynamic and biogeochemical
233 effect on the evolution of phytoplankton communities in the *Ría de Vigo*. Six samples
234 were taken in approximately two weeks corresponding to two different periods
235 (27 September to 8 October 1993, and 6 March to 24 March 1994).

236

237 *Ría de Vigo* 1994-95 (Alvarez et al., 1999; Doval et al., 1998, 1997a, 1997b) and *Ría de*
238 *Vigo* 1997 (Gago et al., 2003a, b, c) were two cruises that took place in the second half
239 of the decade. These campaigns' objective was no longer the ecology of the plankton,

240 but the factors behind the variation of the carbon pools during the upwelling and
241 downwelling events along the central axis of the *Ría of Vigo*. During the 1997 cruises
242 on board the *B/O Mytilus*, a systematic observation of the pCO₂ was carried out for the
243 first time in Spanish coastal waters, using an autonomous continuous system with
244 additional measurements of temperature, salinity and chlorophyll.

245

246 **Cruises in the 2000s and recent years:**

247 After a period of poor sampling at the end of 90s, the first decade of the 21st century
248 gave new impetus to biogeochemical monitoring of Galician waters. As shown below,
249 several projects dealt with various objectives, focussing on particular issues in the
250 dynamics of these waters:

251

252 The DYBAGA project (Galician Platform's Annual Dynamics and Biochemistry: short-
253 scale variation) (Álvarez-Salgado et al., 2006; Castro et al., 2006; Nieto-Cid et al.,
254 2004) analysed the phenomena of upwelling and downwelling in the Galician shelf
255 opposite the *Ría de Vigo* weekly and their impact on the different biogeochemical and
256 carbon system variables including organic dissolved matter. Three stations were
257 sampled weekly from May 2001 to April 2002 between the shelf break (1,200 m deep)
258 to the middle of the *Ría de Vigo* (45 m deep).

259

260 The REMODA (Reactivity of dissolved organic matter in a coastal upwelling system)
261 (Álvarez-Salgado et al., 2005; Piedracoba et al., 2005; Nieto-Cid et al., 2006) project
262 concentrated on learning the origin and destination of dissolved organic matter in the
263 *Ría de Vigo* as well. Three stations along the main axis of the *Ría de Vigo*, including the
264 fixed station as the central one, took samples with short (3-4 days) and seasonal time
265 scales.

266

267 The FLUVBE project (Coupling of benthic and pelagic fluxes in the *Ría de Vigo*) added
268 to knowledge about the productivity and the benthic fluxes of oxygen and inorganic
269 nutrients in the *Ría de Vigo* from 16 oceanographic surveys with four stations between
270 April 2004 and January 2005.

271

272 The ZOTRACOS project studied the biogeochemical and hydrodynamic
273 characterization of the coastal transition zone in NW Spain during the downwelling
274 period (Teira et al., 2009).

275

276 The CRIA (Circulation in a RIA) (Barton et al., 2019) project examined the layout of
277 the two-layer circulation and propagation of upwelled and downwelled waters in order
278 to estimate the flushing and vertical velocities in the *Ría de Vigo* in repeated
279 hydrographic surveys between September 2006 and June 2007 (Barton et al., 2015,
280 2016; Alonso-Perez and Castro, 2014; Alonso-Perez et al., 2010; Alonso-Perez et al.,
281 2015).

282

283 The RAFTING project (Impact of mussel raft cultivation on the benthic-pelagic
284 coupling in a Galician ria) (Frojan et al., 2018; Frojan et al., 2016; Froján et al., 2014)
285 assessed for the first time how mussel cultivation influences the quality of particular
286 organic carbon fluxes in the *Ría de Vigo*. Over the four seasons, two stations were
287 visited every two to three days during each period, meaning 24 oceanographic cruises in
288 2007 and 2008.

289

290 The CAIBEX (Continental shelf-ocean exchanges in the marine ecosystem of the
291 Canary Islands-Iberian Peninsula) (Villacieros-Robineau et al., 2019) project compared
292 the dynamics and biogeochemical activity between the coastal zone and the adjacent
293 ocean in the study zone during the summer upwelling events. As part of the CAIBEX
294 project, a mooring at the LOCO (Laboratory of Ocean and Coastal Observation)
295 (Zuñiga et al., 2016, 2017) site located on the continental shelf was deployed and visited
296 monthly for one year to monitor the vertical profiles of biogeochemical variables.

297

298 After these projects were completed in 2009, new measurements were not provided
299 until 2018. The aim of the ARIOS project (Acidification in the rias and on the Iberian
300 continental shelf) was to evaluate the impact of ocean acidification and learn about
301 potential impacts on the mussels and their adaptation (Lassoued et al., 2019) to the new
302 climate change.

303

304 **3.4. Methods**

305 To assess of the level of acidification in the ocean adjacent to the Galician coast,
306 variables of the carbon system (pH and alkalinity), nutrient concentration, dissolved
307 oxygen, chlorophyll-a, salinity and temperature were measured in each cruise. The
308 variables measured in each oceanographic cruise gathered in the ARIOS dataset are
309 shown in Table 1. The main changes in the material and methods throughout these years
310 are detailed below.

311

312 **T-S measurements**

313 Temperatures from 1976 to 1984 were measured using a Wallace and Tiernan
314 bathythermograph. Reversing thermometers that had a precision of 0.02°C were used,
315 attached to the water samplers between 1984 and 1990, correcting the temperature
316 between the protected and unprotected thermometers according to Anderson (1974).
317 During those years, the depth was calculated from the thermometric readings, rounding
318 the result off to the nearest ten. After 1990, different models of CTD instruments that
319 measured the seawater temperature with a precision of 0.002°C were used to obtain the
320 thermohaline profile.

321

322 The first measurements of salinity were determined with a Plessey Environmental
323 Systems 6230N inductive salinometer calibrated with normal IAPSO water and
324 calculated from the equations given in the NIO and UNESCO International
325 Oceanographic Tables (1981). The precision of these salinity measurements was 0.005
326 psu. After using this equipment, the salinity was determined with an AUTOSAL 8400A
327 inductive salinometer calibrated with normal IAPSO water whose estimated analytical
328 error was 0.003, using the equation of practical salinity, given by UNESCO (1981).

329 CTDs began to be used in 1990 to record the vertical salinity profiles, calibrated using
330 the salinity samples, whose possible deviations in the measurements were estimated
331 from the discrete measurements from the AUTOSAL salinometer.

332

333 **pH measurements**

334 The pH measurements were originally taken with a Metrohm E-510 pH meter with a
335 glass electrode and a Ag/ClAg reference one calibrated with 7.413 NBS buffer. All pH
336 values were converted to values at 15 °C using the temperature correction from the
337 Buch and Nynas tables published by Barnes (1959). In 1984, the method was modified
338 and the temperature normalization was carried out following Pérez and Fraga (1987b).

TONI PADIN 31/7/2020 15:07

Eliminado: psu

TONI PADIN 31/7/2020 15:07

Eliminado: s

341 Two years later, the measurement equipment was the Metrohm E-654 pH meter with an
342 Orion 81-04 Ross combined glass electrode, with the pH converted to the SWS scale
343 using the hydrogen activity coefficient given by Mehrbach et al. (1973) at 25°C with the
344 parameterization given by Pérez and Fraga (1987b). The error in this potentiometric
345 method was 0.010. In 2001, the seawater pH measurements were determined with a
346 spectrophotometric method following Clayton and Byrne (1993), subsequently adding
347 0.0047 to the pH value according to DelValls and Dickson (1998). The precision of the
348 spectrophotometric measurements was 0.003 pH units.

349

350 The pH values were reported on total pH scale at 0 dbar of pressure and both at 25°C
351 and in situ temperature (pH_T) following the same procedure of GLODAP v2 (Olsen et
352 al., 2019). A total of 12,220 measurements of pH on NBS scale were converted to the
353 total scale using CO2SYS (Lewis and Wallace, 1998) for MATLAB (van Heuven et al.,
354 2011) with pH and total alkalinity as inputs. The conversion was conducted with the
355 carbonate dissociation constants of Lueker et al. (2000) and the borate-to-salinity ratio
356 of Uppström (1974). Whenever total alkalinity data were missing, these values were
357 approximated as 66 times salinity that is the mean ratio between the total alkalinity and
358 the salinity of every in situ measurements compiled in the ARIOS database. Data for
359 phosphate and silicate are also needed and were, whenever missing, a constant values of
360 $10 \mu\text{mol kg}^{-1}$ for silicate and $1 \mu\text{mol kg}^{-1}$ for phosphate were used. These
361 approximations were tested on 8,296 samples with complete biogeochemical
362 information showing a bias of less than 0.0004 pH units for 99.95% of the samples.

363

364 **Alkalinity measurements**

365 The seawater alkalinity was measured for the first time in 1981 by potentiometric
366 titration with HCl 0.1M at final pH 4.44 following Pérez and Fraga (1987a) with an
367 analytical error of $2 \mu\text{mol kg}^{-1}$ and a precision of 0.1%. Sodium tetraborate decahydrate
368 (Borax, $\text{Na}_2\text{B}_4\text{O}_7 \cdot 10\text{H}_2\text{O}$, Merck p.a.) was used for standardizing the HCl (0.13 M). The
369 pH measurements were carried out with a combined glass electrode (Metrohm E-121)
370 with Ag/AgCl (KCl 3M) as the reference. The pH was calibrated using the NBS buffers
371 assuming the theoretical slope. As of 2001, the accuracy of alkalinity measurements
372 was determined using samples of certified reference material (CRM) provided by Dr. A.
373 Dickson, University of California, improving the precision to $\pm 1.4 \text{ mol kg}^{-1}$ and an

374 accuracy of <0.1% recently established by (Ríos and Pérez, 1999) from cross-
375 calculation with measured Certified Reference Materials (Dickson et al., 2007).

376

377 **Nutrient measurements**

378 Except for the Galicia cruises (Table 1), in which nutrient samples were analysed on
379 board, samples were kept in the dark and cold (4°C) after collection for further analyses
380 in the shore based laboratory. Nutrient concentration was determined by a flow-
381 segmented autoanalyzer (Technicon AAII and Alpkem after 1995) as described in
382 Strickland and Parsons (1968) with the particularity that the reduction of nitrate to
383 nitrite with Cd column was done using a citrate buffer according to Mouriño and
384 Fraga's modification (1985). Phosphates and silicates were measured following
385 Grasshoff (1983), and ammonium as described by Grasshoff and Johannsen (1972).
386 This method was maintained in the subsequent cruises, achieving a precision of 0.02
387 $\mu\text{mol/kg}$ for nitrite, 0.1 $\mu\text{mol/kg}$ for nitrate, 0.05 $\mu\text{mol kg}^{-1}$ for ammonium and silicate,
388 and 0.01 $\mu\text{mol/kg}$ for phosphate.

389

390 **Oxygen measurements**

391 The dissolved oxygen was determined via the Winkler titration method for the first time
392 in 1981 following the procedure published later by Culbertson et al. (1991). The oxygen
393 concentration in the samples in this method was fixed with MnCl_2 and NaOH/NaI ,
394 which were kept in the dark until analysis in the laboratory 12-24 hours later. The
395 measurements were made by titration of iodine with thiosulfate using an automatic
396 titrator. During the 80s and early 90s, the titration was carried out with Metrohm
397 instruments (E-425 or E-473), which had an analytical error of 1 $\mu\text{mol kg}^{-1}$. The oxygen
398 concentration after 1997 was estimated using a Titrino 720 (Metrohm) analyser with an
399 accuracy of 0.5 $\mu\text{mol kg}^{-1}$.

400

401 **Chlorophyll measurements**

402 The chlorophyll-a values were measured following SCOR-UNESCO (1966) using a
403 6 cm diameter Schleicher and Scholl 602eh filter covered with magnesium carbonate.
404 The absorption was measured in 1 cm optical path cuvettes using a Beckman DU
405 spectrophotometer. In 1984, discrete water samples of the chlorophyll-a samples were
406 filtered through Whatman GF/F filters of 2.5 cm, which were preferred from then on,
407 and measured fluorometrically following Strickland and Parsons (1972) without

408 correction for concentration by pheophytes. The fluorescence readings were carried out
409 with a Turner Designs 10,000 R fluorometer (Yentsh and Menzel, 1963) obtaining a
410 precision of 0.05 g L⁻¹.

411

412 **Quality control**

413 Every cruise gathered in Table 1 passed 1st quality control (QC1) to ensure truly
414 confident results. The GO-SHIP software for quality control of hydrographic data (Velo
415 et al., 2019) that compile several QC1 procedures was applied to ARIOS dataset. That
416 procedures consist on reviewing the property profiles and property-property plots
417 generated by that application, adequate for each variable. A quality control flag value
418 following the recommendations from WOCE bottle data flagging quality codes was
419 assigned to each measurement available from the repository sites (Table 1). This
420 method was preferred over applying a very stringent flagging process because it is
421 difficult to rule out some extreme values associated with low salinities or that could be
422 supported by the high variability of an ecosystem characterized by an intense biological
423 activity. Nutrients and chlorophyll with values inferior to the precision were flag=~~2~~
424 Some very low pH associated to very low salinity waters were flagged as doubtful.

425

426 The ARIOS database includes the cruise corrections for pH data of the -0.017 for the
427 Galicia VIII cruise (29GD19840711) and +0.032 for Galicia IX cruise
428 (29GD19860904) detected during the second level quality control of CARINA project
429 (Velo et al., 2010).

430 **4. Results**

431 Some of the most obvious results provided by the ARIOS database are shown below.
432 The purpose is to describe the environmental context and the main oceanographic
433 processes that affect the variability of these discrete measurements and offer
434 preliminary information for future detailed biogeochemical research.

435

436 **4.1. Vertical distribution**

437 The vertical profile of the temperature, salinity, pH on total scale at in situ temperature
438 (pH_T), NO₃⁻ and oxygen concentration in the ocean region between 41°N and 43°N was
439 estimated for each oceanographic station as the mean value of the depth ranges
440 described in Figure 2b. These measurements were gathered attending to the collection
441 periods (December-February, March-May, June-August and September-November) and

TONI PADIN 3/8/2020 13:07

Eliminado: 6

443 averaged to describe winter, spring, summer and autumn respectively (Fig. 3, [Table A1](#)
444 [in the Appendix](#)).

445

446 The vertical distribution of the temperature (Fig. 3a) showed the presence of warmer
447 saline waters throughout the water column in winter with the exception of the surface
448 waters during summer, which showed intense heating due to the radiant solar energy.
449 Below the maximum temperature observed during the summer, cold central waters of
450 subpolar origin occupied the water columns with lower salinity (Fig. 3b). The vertical
451 variation of temperature is typical for a temperate region with relatively homogenous
452 deep water below the seasonal thermocline, reaching maximum SST values in summer
453 and autumn, and minimums in spring and winter. The winter temperature profile is
454 relatively warmer than in spring because of the presence of the IPC (Alvarez-Salgado et
455 al., 2006), which reaches a depth of 300 metres. The maximum salinity is also found in
456 winter due to the presence of the IPC, whereas the minimum values are found in autumn
457 (Fig. 3b). Below 500 metres in depth, the increase in salinity points to the presence of
458 Mediterranean Water. These differences reach a minimum at 500 metres deep, where
459 the salinity values coincided. From this depth down to 1,100 metres, the differences in
460 temperature and salinity throughout the four seasons were minimal, with the mean
461 values converging to $11.03\pm 0.07^{\circ}\text{C}$ and 36.117 ± 0.009 psu, respectively (Fig. 3ab).

462

463 The vertical profiles of pH_T , NO_3^- and oxygen concentration (Fig. 3cde) also showed a
464 variation lower than 1% within this depth range with annual means of 15.2 ± 0.1 μmol
465 kg^{-1} , 8.025 ± 0.005 and 188 ± 1 $\mu\text{mol kg}^{-1}$ respectively. The pH values from a maximum
466 subsurface located at around 40 metres deep showed a clear inverse correlation with the
467 depth down to a depth of 500 metres throughout the seasonal cycle, where the annual
468 minimum value of 8.018 ± 0.005 was reached. The higher pH values could be attributed
469 to the biological reduction of CO_2 by phytoplankton activity, which brought the pH to a
470 maximum value of 8.13 to 40 meters during the spring bloom. After the intense
471 photosynthetic activity observed in surface waters during spring and summer, pH values
472 reached minimum values in the first 200 metres of depth during autumn due to
473 respiration of organic matter. However, it was at a depth of 500 metres that the
474 minimum pH values were measured in all seasons where is found the subpolar Eastern
475 North Atlantic Central Water proceeding from the northeastern cyclonic gyre (Harvey,
476 1982; Ríos et al., 1992). The influence of phytoplankton growth on biogeochemistry

477 during spring can be also evidenced by the oxygen concentration pattern (Fig. 3e). In
478 the upper layer above 250 metres depth, spring oxygen levels exceeded those in winter,
479 whereas a decrease in oxygen concentration was found from this depth down to 1000
480 metres, possible due to enhanced respiration from cascading organic matter. The impact
481 on the growth of the phytoplankton community during the spring was also evident,
482 judging by the oxygen concentration. So, in the upper waters the spring oxygen
483 concentration values exceeded those of the winter values, while oxygen consumption
484 was found from a depth of 300 metres to 1,000 metres due to respiration from organic
485 matter arriving from above. The minimum values for oxygen concentration throughout
486 the water column were found during summer and autumn. The nitrate concentration
487 displayed a particularly vertical distribution, growing with depth from minimum values
488 in the upper layer of the ocean region, which was practically zero during the first 50
489 metres. Below 100 metres, the nitrate concentration showed the maximum values in the
490 vertical distribution during summer and autumn coinciding with the presence of waters
491 of subpolar and subtropical origin respectively, whereas the minimum values appeared
492 in winter. Towards the bottom, the seasonal values of NO_3^- concentration were almost
493 coincident at a mean value of $15.2 \pm 0.1 \mu\text{mol kg}^{-1}$.

494

495 **4.2. Seasonal cycle**

496 The seasonal cycle of the biogeochemical properties (temperature, salinity, pH_T , oxygen
497 concentration, nitrate concentration and chlorophyll) in the surface waters (0 to 5
498 metres) of five geographical boxes was estimated as a monthly average previously
499 filtering values outside of two standard deviations of the mean ([Table A2 in the](#)
500 [Appendix](#)). Five regions that were located as a longitudinal transect between the inner
501 Ría de Vigo and the ocean zone are shown in Fig. 4.

502

503 In general terms, the seasonal variability of the temperature was very similar in every
504 area, ranging between 12 and 19°C (Fig. 4a). Only particular features observed on a
505 short-term scale as in the examples below differ between each region. The warmer
506 waters were usually found in the oceanic zone, reaching a maximum monthly averaged
507 temperature of 18.6°C in September, while the coldest surface waters of 12.6°C were
508 located in the inner stations closer to the mouth of the *Ría de Vigo* in January. Another
509 secondary minimum averaged temperature was also found in the shelf and the outer area
510 of the *Ría de Vigo*, which was remarkably low in August due to the entry of cold

511 upwelled waters in the surface layer (Alvarez-Salgado 1993).

512

513 The monthly salinity averages (Fig. 4b) clearly showed significant differences between
514 the offshore and coastal waters. Sharp salinity changes were seen in the estuary during
515 winter, especially in the inner area where values lower than 28 psu were reached with
516 the arrival of continental inputs in December. The weak seasonal cycle of salinity in the
517 shelf and ocean waters showed high values in December due to the influence of warm
518 saline water from the IPC, usually located on the shelf slope even though it may even
519 enter the rias depending on the relative intensity of shelf winds and the intensity of the
520 continental runoff (Alvarez-Salgado et al., 2003). In this sense, the slight salinity
521 minimum observed in the shelf waters in March could be consequence of the offshore
522 spreading of the maximum discharges from the River Miño and Douro (Otero et al.,
523 2010) at the end of downwelling season. After this, the shelf and ocean waters showed
524 minimum values in summer due to the arrival of cooler and fresher subpolar waters
525 (Rios et al., 1992; Alvarez-Salgado et al., 2003, 2006). In August, coinciding with the
526 maximum salinity of the surface waters in the interior of the *Ría de Vigo* due to the
527 minimum river runoff, the surface waters between the inner *Ría de Vigo* and the ocean
528 region were almost homogeneous, with minimum differences in salinity of 0.2 psu.

529

530 Like salinity, there was little seasonal variability in pH in the offshore waters, but large
531 seasonal variability in coastal waters, with maximum and minimum pH values in spring
532 and autumn, respectively, and in all regions (Fig. 4c). The net balance between
533 production and respiration of organic matter and the estuarine circulation caused a
534 maximum pH of 8.19 in the outer region of the *Ría de Vigo* in May and a minimum of
535 7.96 in the inner waters in November.

536

537 The oxygen concentration (Fig. 4d) in the coastal ecosystems is also controlled by the
538 remineralization of the organic matter and photosynthetic activity of the phytoplankton
539 community, with the effect of salinity and temperature on the oxygen saturation level.
540 The variability in the oxygen concentration, like the pH distribution, showed a growing
541 seasonal amplitude towards the coastline, with maximum values in the outer and middle
542 *Ría de Vigo* and lower values in the inner waters, especially during the second half of
543 the seasonal cycle. Hence, the dissolved oxygen concentration mirrored the seasonal
544 cycle of pH, showing growing seasonal amplitude towards the coastline with a range

545 between 284 $\mu\text{mol kg}^{-1}$ found in the outer region of the *Ría de Vigo* in May and 205
546 $\mu\text{mol kg}^{-1}$ in the inner waters in November. These results seem to reinforce the
547 importance of the oxygen consumption in this shallow area, where the water column is
548 less than 10 metres deep and therefore it would also be influenced by benthic respiration
549 (Alonso-Pérez and Castro, 2014).

550

551 The monthly means of nitrate concentration (Fig. 4e) could be summarized as high
552 values during autumn and winter due to the nutrients delivered from the continent and
553 the vertical mixing, and as minimum nitrate values from March to September because of
554 phytoplankton consumption. The nitrate concentration was markedly higher in the inner
555 *Ría de Vigo*, where it exceeded 9 $\mu\text{mol kg}^{-1}$ in February and decreased towards the open
556 ocean, where the highest monthly value was seen to be 2.5 $\mu\text{mol kg}^{-1}$. Some notable
557 aspects can be seen in Fig. 5d, such as water poor in nitrate in the ocean region between
558 the two peaks of 3.5 $\mu\text{mol kg}^{-1}$ in March and 1.3 $\mu\text{mol kg}^{-1}$ in October. This shows the
559 presence of the IPC waters, which are warmer and saltier than the shelf waters. Also
560 noteworthy was the particular fact that while the nitrate concentration in other areas was
561 practically zero in summer, the nitrate amount in the surface waters within the *Ría de*
562 *Vigo*, and especially in the inner *Ría de Vigo*, was not completely consumed. This
563 indicates a constant supply throughout the year, either through upwelling events or the
564 continental inputs. This in turn means that while the chlorophyll values were at a
565 minimum in the offshore waters in summer, the phytoplankton community in the
566 estuary grew in summer during the upwelling relaxation periods (Pérez et al., 2000).
567 The nutrient concentration during spring and summer was only detectable in the newly
568 upwelled waters that can show values up to 6 $\mu\text{mol L}^{-1}$ (Fraga, 1981; Castro et al.,
569 1994). During the cessation of the upwelling season in September and October, the
570 chlorophyll concentration (Fig. 5f) increased again, sustained by nutrients that entered
571 from deeper waters through vertical mixing. It should be noted that there was a
572 coincidence of high chlorophyll in the water column and low oxygen concentration in
573 the inner *Ría de Vigo* from May to November, indicating the potential importance of
574 benthic fluxes and vertical fluxes (reference).

575

576 **4.3. Long-term trends**

577 The long-term trends of the biogeochemical properties in the surface waters along the
578 described longitudinal transect between the inner *Ría de Vigo* and the ocean zone were

579 estimated to be the interannual linear rate of the deseasonalized time series, previously
580 removing the monthly means in these regions and assuming a null spatial variability.
581 The significant trends in the ARIOS database, meaning long-term variability, should be
582 interpreted as a combination of the natural variability on a decadal scale (Pérez et al.,
583 2010; Padin et al., 2010) and anthropogenic forcings (Wolf-Gladrow et al., 1999;
584 Anderson and Mackenzie 2004; Bakun et al., 2010).

585

586 No long-term temperature variability was found in the surface waters of any region
587 despite the known warming previously reported on the Northern Iberian coast (Pérez et
588 al., 2010; Gesteira et al., 2011; González-Pola et al., 2005). Unlike the temperature, the
589 other expected consequence of climate change in marine ecosystems, namely ocean
590 acidification (Caldeira and Wickett, 2003) was observed along the longitudinal transect,
591 with a greater decrease in the long-term trend of pH towards the coast (Table 2). The
592 long-term pH variation of $-0.0039 \pm 0.0005 \text{ yr}^{-1}$ in the inner waters was about three fold
593 higher than the change observed in the ocean zone, equivalent to $-0.0012 \pm 0.0002 \text{ yr}^{-1}$
594 in the ocean zone, explaining the 34% and 22% variation in pH in situ respectively, and
595 representing 1-3% of the seasonal pH variation in all zones. These pH decrease rates
596 found in both coastal and open ocean regions of the Iberian Upwelling System lie
597 within the range of other acidification rates estimated in different sites of the North
598 Atlantic Ocean (Lauvset and Gruber, 2014; Bates et al., 2014), being also coherent with
599 the mean rates calculated for the global ocean and for the Eastern North Atlantic and
600 equal to -0.018 and $-0.0164 \text{ decade}^{-1}$, respectively (Lauvset et al., 2015; Rios et al
601 2001).

602

603 The long-term trend in salinity was also seen to be evidently dependent on the distance
604 to the mouth of the *Ría de Vigo*. The interannual rate of sea surface salinity in the outer
605 and inner ria previously reported by Rosón et al. (2009) was $0.0426 \pm 0.016 \text{ psu yr}^{-1}$ and
606 $0.0193 \pm 0.0056 \text{ psu yr}^{-1}$ respectively. These changes were observed in parallel to an
607 interannual alkalinity increase that is cancelled out in the normalized alkalinity,
608 estimated as the difference between the alkalinity measured and the alkalinity calculated
609 using the linear regression with salinity in each region. Therefore, the interannual
610 salinity increase was the forcing that explains the increase in the buffer capacity of the
611 surface waters (Sarmiento and Gruber, 2006).

612

613 Other significant long-term variations were found in other biogeochemical parameters
614 in the ARIOS database. The long-term trend of the concentrations of nutrients in the
615 inner Ría de Vigo that had been previously reported for the period 2001-2011 by Doval
616 et al. (2016) showed a significant increase in nitrate, phosphate and ammonium
617 concentrations of $0.0559 \pm 0.0158 \mu\text{mol kg}^{-1} \text{ yr}^{-1}$, $0.0076 \pm 0.0016 \mu\text{mol kg}^{-1} \text{ yr}^{-1}$ and
618 $0.0560 \pm 0.0011 \mu\text{mol kg}^{-1} \text{ yr}^{-1}$ respectively. This fertilization on a long-term scale in the
619 surface waters of the inner ria estimated from ARIOS database was observed in parallel
620 to the deoxygenation of $-0.7 \pm 0.2 \mu\text{mol kg}^{-1} \text{ yr}^{-1}$. The apparent oxygen utilisation
621 (AOU), calculated using the concentration of O_2 at saturation calculated according to
622 Benson and Krause (1984), underwent an equivalent significant long-term change of
623 $0.7 \pm 0.2 \mu\text{mol kg}^{-1} \text{ yr}^{-1}$, indicating that either the biological consumption rates, or a
624 change in the amount of time that the waters are ventilated, or even its interaction or
625 exchange with the sediment, cause the the long-term reduction of oxygen.

626

627 This fertilization on a long-term scale estimated from ARIOS database in the surface
628 waters of the inner ria was observed in parallel to the deoxygenation of $-0.7 \pm 0.2 \mu\text{mol}$
629 $\text{kg}^{-1} \text{ yr}^{-1}$. The apparent oxygen utilisation (AOU), calculated using the concentration of
630 oxygen at saturation calculated according to Benson and Krause (1984), underwent a
631 long-term change of $0.7 \pm 0.2 \mu\text{mol kg}^{-1} \text{ yr}^{-1}$ equal to the observated in the measurements
632 of oxygen concentration. This coincidence may indicates that the long-term reduction of
633 oxygen is due to the changes in the biological consumption rates, in the rates of the
634 waters ventilation or even in sediment-water interactions rather than due to the effect of
635 temperature. and salinity on oxygen saturation.

636

637 These findings found in the shallower waters of the *Ría de Vigo* allow us to hypothesize
638 that the long-term increase in salinity would produce an increasingly weak vertical
639 salinity gradient in the water column that would favour the vertical fluxes between the
640 bottom and surface waters. Therefore the observed changes of oxygen and
641 remineralized nutrient inputs in the surface waters could be due to an increasing
642 footprint of benthic respiration, that has a major importance in the net ecosystem
643 metabolism of this coastal region (Alonso-Pérez et al., 2015). This hypothesis would
644 also explain the intense acidification in the inner waters in spite of growing alkalinity
645 buffering.

646

647 The mean values at each station of the ARIOS database estimated for each depth range
648 described in Figure 2, resulting in 8,384 values, were used to estimate a general value of
649 the long-term trend in pH. The historical pH values in situ from the ARIOS database
650 showed a general decrease in seawater pH in the Iberian Upwelling between 1976 and
651 2018, with an acidification rate of $-0.012 \pm 0.002 \text{ yr}^{-1}$ that significantly explains 2% of
652 the total pH variation (Fig. 5a). The apparent oxygen utilisation was also shown as
653 function of pH over time, revealing the association of higher AOU values with lower
654 pH. The relationship between pH and AOU (Fig. 5b) showed an inverse linear
655 correlation of $-399 \pm 5 \mu\text{mol kg}^{-1}$ and a coefficient of determination (r-squared) of 0.52.
656 The strong biological activity of the upwelling systems is the main driver of pH
657 changes, explaining 52% of the observed variation in the discrete measurements. The
658 distribution of nitrate seen in relation to the distribution of pH and AOU (Fig. 5b)
659 showed the association of higher pH values with negative AOU values and a nitrate
660 decrease, reinforcing the importance of biological processes in these marine carbonate
661 system. Although the different processes controlling the AOU values were not separated
662 in this analysis, the oxygen concentration in addition to the remineralization of the
663 organic matter and the photosynthesis is conditioned by changes in temperature and
664 salinity, ventilation events, water masses mixing and other processes (Sarmiento and
665 Gruber, 2006). Therefore, the long-term drop in seawater pH measurements estimated
666 from the ARIOS database presented here confirms that the future evolution of ocean
667 acidification in this productive region is likely to depend on both the CO_2 increase in
668 the atmosphere and other long-term changes (of natural and/or anthropogenic origin)
669 affecting the seawater's carbonate system.

670

671 **5. Data availability**

672 The ARIOS dataset (Pérez et al., 2020) is archived at DIGICAL CSIC under the Digital
673 Object Identifier (DOI): <http://dx.doi.org/10.20350/digitalCSIC/12498>.

674

675 The data are available as WHP-Exchange bottle format (arios_database_hy1.csv). A
676 documentation file (readme_ARIOSDATABASE.txt) provides an description of the
677 material and methods of the measurements and the parameters of the dataset. In both
678 files, a table similar to the Table 1 of this manuscript include the DOI and the
679 EXPOCODE of the original cruise files gathered in the ARIOS dataset.

680

681 These data are available to the public and the scientific community with the aim of that
682 their wide dissemination will lead to new scientific knowledge about the ocean
683 acidification and the biogeochemistry of the Galicia Upwelling System. The dataset is
684 subject to a Creative Commons License Attribution-ShareAlike 4.0 International
685 (<http://creativecommons.org/licenses/by-sa/4.0/>) and users of the ARIOS dataset should
686 reference this work.

687

688 **6. Conclusions**

689 The ARIOS database is a unique compilation of biogeochemical discrete measurements
690 in the Iberian Upwelling Ecosystem from 1976 to 2018. This data set comprises more
691 than 17,653 discrete samples from 3,357 oceanographic stations (but not always for all
692 parameters) of pH, alkalinity and associated physical and biogeochemical parameters
693 (e.g., temperature, salinity, and chlorophyll and oxygen concentrations). The material
694 and methods varied throughout the sampling period due to logistical and analytical
695 issues such as those described in Table 1, where different sites are mentioned to
696 download these measurements and detailed information.

697

698 Among the results described as preliminary and relevant information to learn the
699 environmental and oceanographic context of the ARIOS database, we can mention the
700 following main points concerning the pH characteristics of the Iberian Upwelling
701 System:

- 702 • A decrease in seawater pH in the Iberian Upwelling between 1976 and 2018,
703 with an acidification rate of $-0.012 \pm 0.002 \text{ yr}^{-1}$ that significantly explains 2% of
704 the total pH variation
- 705 • An interannual pH variation of $-0.0039 \pm 0.0005 \text{ yr}^{-1}$ in the inner waters and -
706 $0.0012 \pm 0.0002 \text{ yr}^{-1}$ in the ocean zone.
- 707 • An inverse linear correlation between pH and AOU of $-399 \pm 5 \text{ } \mu\text{mol kg}^{-1}$ that
708 explained 52% of the observed variation in the discrete measurements.

709

710 This published ARIOS database is a useful and necessary tool to confirm and study
711 biogeochemical changes in the seawater at long term trend. Likewise, we understand
712 that it is a starting point to which to add future observation projects to continue
713 increasing the knowledge about the impact of climate change in the Iberian Upwelling
714 Ecosystem.

715

716 **Acknowledgements.**

717 The compilation of this data set was funded by the ARIOS project (CTM2016-76146-
718 C3-1-R) funded by the Spanish government through the Ministerio de Economía y
719 Competitividad that included European FEDER funds. Part of the processing work was
720 supported by the MarRISK project (European Union FEDER 0262_MarRISK_1_E)
721 funded by the Galicia-Northern Portugal Cross-Border Cooperation Program
722 (POCTEP). This project has also received funding from the European Union's Horizon
723 2020 research and innovation programme under grant agreement No 820989 (project
724 COMFORT, Our common future ocean in the Earth system – quantifying coupled
725 cycles of carbon, oxygen, and nutrients for determining and achieving safe operating
726 spaces with respect to tipping points). This data set encompasses decades of work
727 conducted by an overwhelming number of people. We thank all of the scientists,
728 technicians, personnel, and crew who were responsible for the collection and analysis of
729 the over 22 000 samples included in the final data set. In addition to the PI cited in
730 Table 1 we also thank to Trinidad Rellán, Antón Velo, Miguel Gil Coto, Marta Alvarez,
731 Marylo Doval, Jesus Gago, Daniel Broullón and Marcos Fontela. We also thank Monica
732 Castaño for starting this data compilation more than 10 years ago.

733

734 **References**

735 Alonso-Perez F., Ysebaert, T., and Castro, C. G.: Effects of suspended mussel culture
736 on benthic-pelagic coupling in a coastal upwelling system (Ría de Vigo, NW Iberian
737 Peninsula), *Journal of Experimental Marine Biology and Ecology*, 382–391,
738 <https://doi.org/10.1016/j.jembe.2009.11.008>, 2010.

739

740 Alonso-Perez, F., and Castro, C. G.: Benthic oxygen and nutrient fluxes in a coastal
741 upwelling system (Ria de Vigo, NW Iberian Peninsula): seasonal trends and regulating
742 factors. *Mar Ecol Prog Ser* 511:17-32. <https://doi.org/10.3354/meps10915>. 2014.

743

744 Alonso-Perez, F., Zúñiga, D., Arbones, B., Figueiras, F. G., and Castro, C. G.: Benthic
745 fluxes, net ecosystem metabolism and seafood harvest: Completing the organic carbon
746 balance in the Ría de Vigo (NW Spain), *Estuarine Coastal Shelf Science*, 163,
747 <https://doi.org/10.1016/j.ecss.2015.05.038>. 2015.

748

749 Alvarez-Salgado, X. A., Rosón, G., Pérez, F. F. and Pazos, Y.: Hydrographic variability
750 off the Rías Baixas (NW Spain) during the upwelling season. *Journal of Geophysical*
751 *Research* 98, 14447–14455, 1993.

752

753 Alvarez-Salgado, X. A., Figueiras, F. G., Villarino, M. L., and Pazos, Y.:
754 Hydrodynamic and chemical conditions during onset of a red-tide assemblage in an
755 estuarine upwelling ecosystem, *Marine Biology*, 130, 509–519, 1998.

756

757 Alvarez, M., Fernández, E., and Pérez, F. F.: Air-sea CO₂ fluxes in a coastal embayment
758 affected by upwelling: physical versus biological control, *Oceanologica Acta*, 22, 5,
759 499–515, 1999.

760

761 Álvarez-Salgado, X. A., Doval, M.D., Borges, A.V, Joint, I., Frankignoulle, M.,
762 Woodward, E.M.S., and Figueiras, F.G.: Off-shelf fluxes of labile materials by an
763 upwelling filament in the NW Iberian Upwelling System, *Prog. Oceanogr.*, 51(2–4),
764 321–337, 2001.

765

766 Álvarez-Salgado, X. A., Beloso, X., Joint, I., Nogueira, E., Chou, L., Pérez, F. F.,
767 Groom, S., Cabanas, J. M., Rees, A.P., and Elskens, M.: New Production of the NW
768 Iberian Shelf during the Upwelling Season over the period 1982-1999. *Deep-Sea Res.*
769 49(10), [http://dx.doi.org/10.1016/S0967-0637\(02\)00094-8](http://dx.doi.org/10.1016/S0967-0637(02)00094-8), 2002.

770

771 Álvarez- Salgado, X. A., Figueiras, F. G., Pérez, F. F., Groom, S., Nogueira, E., Borges,
772 A. V., Chou, L., Castro, C. G., Moncoiffé, G., Ríos, A. F., Miller, A.E.J., Frankignoulle,
773 M., Savidge, G., and Wollast, R.: The Portugal coastal counter current off NW Spain
774 new insights on its biogeochemical variability, *Progress in Oceanography*, 56(2)
775 [http://dx.doi.org/10.1016/S0079-6611\(03\)00007-7](http://dx.doi.org/10.1016/S0079-6611(03)00007-7), 2003.

776

777 Álvarez-Salgado, X. A., Nieto-Cid, M., Piedracoba, S., Crespo, B. G., Gago, J., Brea,
778 S., Teixeira, I. G., Figueiras, F. G., Garrido, J. L., Rosón, G., Castro, C. G., and Gilcoto,
779 M.: Origin and fate of a bloom of *Skeletonema costatum* during a winter
780 upwelling/downwelling sequence in the Ría de Vigo (NW Spain), *Journal of Marine*
781 *Research*, 63, 6, 1127–1149, <http://dx.doi.org/10.1357/002224005775247616>, 2005.

782

783 Alvarez-Salgado, X. A., Nieto-Cid, M., Gago, J., Brea, S., Castro, C. G., Doval, M., and
784 Pérez, F. F.: Stoichiometry of the degradation of dissolved and particulate biogenic
785 organic matter in the NW Iberian upwelling, *Journal of Geophysical Research*, 111,
786 C07017, <http://dx.doi.org/10.1029/2004JC002473>, 2006.
787
788 Anderson, L.: Correction of reversing thermometers and related depth calculations in
789 Baltic water, *Meddelande fran Havsfiskelaboratoriet. Lysekil*, 166, 1974.
790
791 Andersson, A. J., and Mackenzie, F. T.: Revisiting four scientific debates in ocean
792 acidification research, *Biogeosciences*, 9, 893–905, [ww.biogeosciences.net/9/893/2012/](http://www.biogeosciences.net/9/893/2012/),
793 2012.
794
795 Arístegui J., Barton, E. D., Tett, P., Montero, M. F., García-Muñoz, M., Basterretxea,
796 G., Cussatlegras, A. S., Ojeda, A., and de Armas, D.: Variability in plankton community
797 structure, metabolism, and vertical carbon fluxes along an upwelling filament (Cape
798 Juby, NW Africa), *Prog. Oceanogr.*, 62 (2-4), 95–113, 2004.
799
800 Bakun, A., Field, D. B., Redondo-Rodriguez, A., and Weeks, S. J.: Greenhouse gas,
801 upwelling favorable winds, and the future of coastal ocean upwelling ecosystems.
802 *Global Change Biology*, 16, 4, 1213–1228, <https://doi.org/10.1111/j.1365->
803 [2486.2009.02094.x](https://doi.org/10.1111/j.1365-2486.2009.02094.x), 2010.
804
805 Barnes, H.: *Apparatus and methods of oceanography. Part one: Chemical*, Allen and
806 Unwin. London, 335 p., 1959.
807
808 Barton, E. D., Largier, J. L., Torres, R., Sheridan, M., Trasviña, A., Souza A., Pazos,
809 Y., and Valle-Levinson, A.: Coastal upwelling and downwelling forcing of circulation
810 in a semi-enclosed bay: Ria de Vigo, *Progress in Oceanography*, 134, 173–189.
811 <https://doi.org/10.1016/j.pocean.2015.01.014>, 2015.
812
813 Barton, E. D., Torres, R., Figueiras, F. G., Gilcoto, M., and Largier, J.: Surface water
814 subduction during a downwelling event in a semienclosed bay, *Journal Geophys.*
815 *Research*, 121, 7088–7107, <https://doi.org/10.1002/2016JC011950>, 2016.
816

817 Barton, E. D., Castro, C. G., Alonso-Pérez, F., Zúñiga, D., Rellán, T., Arbones, B.,
818 Castaño, M., Gilcoto, M., Torres, R., Figueiras, F. G., Pérez, F. F. and Ríos, A. F.: Cria
819 surveys: hydrographic and chemical data, Digital.CSIC,
820 <http://dx.doi.org/10.20350/digitalCSIC/9931>, 2019.
821

822 Bates, N. R., Astor, Y. M., Church, M. J., Currie, K., Dore, J. E., González-Dávila, M.,
823 Lorenzoni, L., Muller-Karger, F., Olafsson, J., and Santana-Casiano, J. M.: A Time-
824 Series View of Changing Surface Ocean Chemistry Due to Ocean Uptake of
825 Anthropogenic CO₂ and Ocean Acidification, *Oceanography*, 27, 1, SPECIAL ISSUE
826 ON Changing Ocean Chemistry, pp. 126–141, Published by: Oceanography Society
827 <https://www.jstor.org/stable/24862128>. 2014.
828

829 Benson, B. B., and Krause, D. J.: The concentration and isotopic fractionation of
830 oxygen dissolved in fresh water and seawater in equilibrium with the atmosphere.
831 *Limnology and Oceanography*, 29(3), 620–632, 1984.
832

833 Blanton, J. O., Atkinson, L. P., Fernandez de Castillejo, F., and Lavin Montero, A.:
834 Coastal upwelling off the Rias Bajas, Galicia, Northwest Spain, I: Hydrography studies.
835 *Rapports et Proc-verbeaux Reun. Cons. into Explor. Mer*, 183, 79–90, 1984.
836

837 Bode, A., Alvarez-Ossorio, M. T., Cabanas, J. M.: Miranda, A., Varela, M.: Recent
838 trends in plankton and upwelling intensity off Galicia (NW Spain), *Progress in*
839 *Oceanography*, 83, 342–350, 2009.
840

841 Caldeira, K., and Wickett, M.E.: *Oceanography: anthropogenic carbon and ocean*
842 *pH*, *Nature*, 425, 365, <https://doi.org/10.1038/425365a>, 2003.
843

844 Castro, C. G., Pérez, F. F., Álvarez-Salgado, X. A., Rosón, G., and Ríos, A. F.:
845 Hydrographic conditions associated with the relaxation of an upwelling event off the
846 Galician coast (NW Spain), *Journal of Geophysical Research*, 99, C3, 5135–5147,
847 <https://agupubs.onlinelibrary.wiley.com/doi/10.1029/93JC02735>, 1994.
848

849 Castro, C. G., Nieto-Cid, M., Álvarez-Salgado, X. A., and Pérez, F. F.: Local
850 remineralization patterns in the mesopelagic zone of the ENAW, *Deep Sea Research*
851 *Part I*, 53 (12), 1925–1940, <http://dx.doi.org/10.1016/j.dsr.2006.09.002>, 2006.
852

853 Castro, C. G., Álvarez-Salgado, X. A., Nogueira, E., Gago, J., Pérez, F. F., Bode, A.,
854 Ríos, A. F., Rosón, G., and Varela, M.: Evidencias bioquímicas do cambio
855 climático. Edita: Xunta de Galicia. Consellería de Medio Ambiente e Desenvolvemento
856 Sostible, *Evidencias e impactos do cambio climático en Galicia*, 303–326, 2009.
857

858 Clayton, T. D., and Byrne, R. H.: Spectrophotometric seawater pH measurements: total
859 hydrogen ion concentration scale calibration of m-cresol purple and at-sea results, *Deep*
860 *Sea Research I*, 40, 10, 2115–2129, [https://doi.org/10.1016/0967-0637\(93\)90048-8](https://doi.org/10.1016/0967-0637(93)90048-8),
861 1993.
862

863 Cobo-Viveros, A. M., Padin, X. A., Otero, P., de la Paz, M., Ruiz-Villareal, M., Ríos,
864 A. F., Pérez, F. F.: Short-term variability of surface carbon dioxide and sea-air CO₂
865 fluxes in the shelf waters of the Galician coastal upwelling system, *Scientia Marina*,
866 77S1, doi: 10.3989/scimar.03733.27C, 2013.
867

868 Culberson, C. H., Knapp, G., Stalcup, M. C., Williams, R. T., and Zemlyak, F.: A
869 comparison of methods for the determination of dissolved oxygen in seawater. WOCE
870 Report 73/91, 77 pp, 1991.
871

872 DelValls, T. A., and Dickson, A. G.: The pH of buffers based on 2-amino-2-
873 hydroxymethyl-1,3-propanediol (“tris”) in synthetic sea water, *Deep-Sea Res. I*, 45,
874 1541–1554, 1998.
875

876 Dickson, A.G., Sabine, C.L., and Christian, J.R.: Guide to best practices for ocean CO₂
877 measurements. PICES Special Publication 3, 191 pp, 2007.
878

879 Doval, M., Nogueira, E., and Pérez, F. F.: Spatio-temporal variability of the
880 thermohaline and biogeochemical properties and dissolved organic carbon in a coastal
881 embayment affected by upwelling: the Ría de Vigo (NW Spain). *Journal of Marine*
882 *Systems*, 14, 1-2, 135–150, [https://doi.org/10.1016/S0924-7963\(97\)80256-4](https://doi.org/10.1016/S0924-7963(97)80256-4), 1998.

883
884 Doval, M. D., Alvarez-Salgado, X. A., and Perez, F. F.: Dissolved organic carbon in a
885 temperate embayment affected by coastal upwelling, *Mar. Ecol. Prog. Ser.*, 157, 21–37,
886 doi:10.3354/meps157021, 1997a.
887
888 Doval, M. D., Fraga, F. and Perez, F.F.: Determination of dissolved organic nitrogen in
889 seawater using Kjeldahl digestion after inorganic nitrogen removal, *Oceanol. Acta.*
890 <https://archimer.ifremer.fr/doc/00093/20429/18096.pdf>, 1997b.
891
892 Doval, M.D., López, A., and Madriñán, M.: Temporal variation and trends of inorganic
893 nutrients in the coastal upwelling of the NW Spain (Atlantic Galician rías),
894 *Journal of Sea Research*, 108, 19–29, <https://doi.org/10.1016/j.seares.2015.12.006>,
895 2016.
896
897 Fraga F.: Upwelling off the Galician coast, northwest Spain. *Coastal Upwelling*,
898 American Geophysical Union, Washington DC, pp. 176–182,
899 <https://doi.org/10.1029/CO001p0176>, 1981.
900
901 Fraga, F., Mouriño, C., and Manriquez, M.: Las masas de agua en la costa de Galicia:
902 junio-octubre. *Result. Exped. Cient. Supl. Invest. Pesq.*, 10, 51–77,
903 <http://hdl.handle.net/10261/90380>, 1982.
904
905 Fraga, F., Pérez, F. F., Figueiras, F. G., and Ríos, A. F.: Stoichiometric variations of N,
906 P, C and O₂ during a *Gymnodinium catenatum* red tide and their interpretation, *Marine*
907 *Ecology Progress Series*, 87, 1-2, 123–134, doi:10.3354/meps087123, 1992.
908
909 Figueiras, F. G., Jones, K., Mosquera, A. M., Álvarez Salgado, X. A., Edwards, A. and
910 MacDougall, N.: Red tide assemblage formation in an estuarine upwelling ecosystem:
911 Ría de Vigo, *Journal of Plankton Research*, 16 (7), 857–878,
912 <https://doi.org/10.1093/plankt/16.7.857>, 1994.
913
914 Froján, M., Arbones, B., Zúñiga, D., Castro, C. G., and Figueiras, F. G.: Microbial
915 plankton community in the Ría de Vigo (NW Iberian upwelling system): impact of the

916 culture of *Mytilus galloprovincialis*, *Mar Ecol Prog Ser*, 498, 43–54,
917 <https://doi.org/10.3354/meps10612>, 2014.

918

919 Froján, M., Figueiras, F. G., Zúñiga, D., Alonso-Pérez, F., Arbones, B., and Castro, C.
920 G.: Influence of Mussel Culture on the Vertical Export of Phytoplankton Carbon in a
921 Coastal Upwelling Embayment (Ría de Vigo, NW Iberia), *Estuaries and Coasts*, 39,
922 1449–1462, <https://doi.org/10.1007/s12237-016-0093-1>, 2016.

923

924 Froján, M., Castro, C. G., Zúñiga, D., Arbones, A., Alonso-Pérez, F., and Figueiras, F.
925 G.: Mussel farming impact on pelagic production and respiration rates in a coastal
926 upwelling embayment (Ría de Vigo, NW Spain), *Estuarine, Coastal and Shelf Science*,
927 204, 130–139, <https://doi.org/10.1016/j.ecss.2018.02.025>, 2018.

928

929 Frouin, R., Fiúza, A. F. G., Ambar, I., and Boyd, T. J.: Observations of a poleward
930 surface current off the coasts of Portugal and Spain during winter, *Journal of*
931 *Geophysical Research*, 95, 679–691, 1990.

932

933 Feely, R. A., Sabine, C. L., Hernandez-Ayon, J. M., Ianson, D., and Hales, B: Evidence
934 for upwelling of corrosive “acidified” water onto the continental shelf, *Science*
935 320(5882), 1490–1492, doi:10.1126/science.1155676, 2008.

936

937 Gago, J., Alvarez-Salgado, X. A., Gilcoto, M., and Pérez, F. F.: Assessing the
938 contrasting fate of dissolved and suspended organic carbon in a coastal upwelling
939 system (Ría de Vigo, NW Iberian Peninsula), *Estuarine, Coastal and Shelf Science*, 56,
940 2, 271–279, [http://dx.doi.org/10.1016/S0272-7714\(02\)00186-5](http://dx.doi.org/10.1016/S0272-7714(02)00186-5), 2003a.

941

942 Gago, J., Alvarez-Salgado, X. A., Pérez, F. F., and Ríos, A. F.: Partitioning of physical
943 and biogeochemical contributions to short-term variability of pCO₂ in a coastal
944 upwelling system a quantitative approach, *Marine Ecology Progress*, 255, 43–54,
945 <http://dx.doi.org/10.3354/meps25504>, 2003b.

946

947 Gago, J., Gilcoto, M., Pérez, F. F., and Ríos, A.F.: Short-term variability of fCO₂ in
948 seawater and air-sea CO₂ fluxes, *Marine Chemistry*, 80, 4, 247–264,
949 [http://dx.doi.org/10.1016/S0304-4203\(02\)00117-2](http://dx.doi.org/10.1016/S0304-4203(02)00117-2), 2003c.

950
951 Gilcoto, M., Largier, J. L., Barton, E. D., Piedracoba, S., Torres, R., Graña, R., Alonso-
952 Pérez, F., Villacieros-Robineau, N., and de la Granda, F.: Rapid response to coastal
953 upwelling in a semienclosed bay, *Geophysical Research Letters*, 44(5), 2388–2397, doi:
954 10.1002/2016GL072416, 2017.

955
956 González-Pola, C., Lavín, A., Vargas-Yáñez, M.: Intense warming and salinity
957 modification of intermediate water masses in the southeastern corner of the Bay of
958 Biscay for the period 1992–2003, *Journal of Geophysical Research*, 110, C05020,
959 doi:10.1029/2004JC002367, 2005.

960
961 Grasshoff, K., Johannsen, H.: A New Sensitive and Direct Method for the Automatic
962 Determination of Ammonia in Sea Water, *ICES Journal of Marine Science*, 34(3), 516–
963 521, <https://doi.org/10.1093/icesjms/34.3.516>, 1972.

964
965 Grasshoff, K., Ehrhardt, M., Kremling, K.: *Methods of Seawater Analysis*, 2nd. ed.
966 Verlag Chemie, Weinheim, 419 pp, 1983.

967
968 Gruber, N., Hauri, C., Lachkar, Z., Loher, D., Frolicher, T. L., and Plattner, G. K.:
969 Rapid progression of ocean acidification in the California Current System, *Science*, 337,
970 220–223, doi:10.1126/science.1216773, 2012.

971
972 Harvey, J.: θ -S relationship and water masses in the eastern North Atlantic. *Deep-Sea*
973 *Research*, 29, 1021-1033, 1982.

974
975 Hauri, C., Gruber, N., Plattner, G. K., Alin, S., Feely, R. A., Hales, B., and Wheeler,
976 P. A.: Ocean acidification in the California Current System, *Oceanography*, 22, 58–69,
977 doi:10.5670/oceanog.2009.97, 2009.

978
979 Hauri, C., Gruber, N., Vogt, M. S., Doney, C., Feely, R. A., Lachkar, Z., Leinweber, A.,
980 McDonnell, A. M. P., Munnich, M., and Plattner, G.K.: Spatiotemporal variability and
981 long-term trends of ocean acidification in the California Current System,
982 *Biogeosciences*, 10, 193–216, doi:10.5194/bg-10-193-2013, 2013.

983 Hofmann, G. E.: High-frequency dynamics of ocean pH: A multi-ecosystem
984 comparison, PLoS One, 6(12), e28983, doi:10.1371/journal.pone.0028983, 2011.
985
986 IPCC: Climate Change 2013: the physical science basis Contribution of Working Group
987 I to the Fifth Assessment Report of the Intergovernmental Panel on Climate Change ed
988 T F Stocker et al (Cambridge: Cambridge University Press) pp 1535,
989 www.ipcc.ch/report/ar5/wg1/, 2013.
990
991 Lachkar, Z.: Effects of upwelling increase on ocean acidification in the California and
992 Canary Current systems, Geophys. Res. Lett., 41, 90–95, doi:10.1002/2013GL058726,
993 2014.
994
995 Lassoued, J., Babarro, J., Padín, X. A., Comeau, L., Bejaoui, N., and Pérez, F.:
996 Behavioural and eco-physiological responses of the mussel *Mytilus galloprovincialis*
997 to acidification and distinct feeding regimes, Marine Ecology Progress Series, 626, 97–
998 108, doi: 10.3354/meps13075, 2019.
999
1000 Lauvset, S.K., and Gruber, N.: Long-term trends in surface ocean pH in the North
1001 Atlantic, Marine Chemistry, 162, 71–76,
1002 <https://doi.org/10.1016/j.marchem.2014.03.009>, 2014.
1003
1004 Lauvset, S. K., Gruber, N., Landschützer, P., Olsen, A., and Tjiputra, J.: Trends and
1005 drivers in global surface ocean pH over the past 3 decades, Biogeosciences, 12(5),
1006 1285–1298, doi:10.5194/bg-12-1285-2015, 2015.
1007
1008 Lewis, E., Wallace, D.W.R.: Program developed for CO₂ system calculations,
1009 ORNL/CDIAC-105, Carbon Dioxide Information Analysis Center, Oak Ridge National
1010 Laboratory, Oak Ridge, TN, USA, 1998.
1011
1012 Lemos, R. T., and Sansó, B.: Spatio-temporal variability of ocean temperature in
1013 the Portugal Current System, Journal of Geophysical Research, 111, C04010,
1014 doi:10.1029/2005JC003051, 2006.
1015

1016 Lueker, T. J., Dickson, A. G., and Keeling, C. D.: Ocean pCO₂ calculated from
1017 dissolved inorganic carbon, alkalinity, and equations for K-1 and K-2: validation based
1018 on laboratory measurements of CO₂ in gas and seawater at equilibrium, *Mar. Chem.*,
1019 70, 105–119, 2000.

1020

1021 McElhany, P. and Shallin Busch, D.: Appropriate pCO₂ treatments in ocean
1022 acidification experiments, *Marine Biology*, 160, 1807–1812,
1023 <https://doi.org/10.1007/s00227-012-2052-0>, 2013.

1024

1025 Mehrbach, C., Culberson, C. H., Hawley, J. E., and Pytlowicz, R. M.: Measurements of
1026 the apparent dissociation constant of carbonic acid in seawater at atmospheric pressure,
1027 *Limnology and Oceanography*, 18, 897–907, 1973.

1028

1029 Miguez, B. M., Fariña-Busto, L., Figueiras, F. G., Pérez, F. F.: Succession of
1030 phytoplankton assemblages in relation to estuarine hydrodynamics in the Ria de Vigo,
1031 *Scientia Marina*, 65, S1, <https://doi.org/10.3989/scimar.2001.65s165>, 2001.

1032

1033 Mouriño, C., and Fraga, F.: Determinación de nitratos en agua de mar, *Investigaciones*
1034 *Marinas*, 49 (1), 81–96, 1985.

1035

1036 Nieto-Cid, M., Alvarez-Salgado, X. A., Brea, S., and Pérez, F. F.: Cycling of dissolved
1037 and particulate carbohydrates in a coastal upwelling system (NW Iberian Peninsula),
1038 [doi:10.3354/meps283039](https://doi.org/10.3354/meps283039), 2004.

1039

1040 Nieto-Cid, M., Alvarez-Salgado, X. A., and Pérez, F. F.: Microbial and photochemical
1041 reactivity of fluorescent dissolved organic matter in a coastal upwelling system
1042 <https://doi.org/10.4319/lo.2006.51.3.1391>, 2006.

1043

1044 Nogueira, E., Pérez, F. F., and Ríos, A. F.: Seasonal and long-term trends in an
1045 estuarine upwelling ecosystem (Ría de Vigo, NW Spain), *Estuarine, Coastal and Shelf*
1046 *Science* 44, 285–300, 1997.

1047

1048 Olsen, A., Lange, N., Key, R. M., Tanhua, T., Álvarez, M., Becker, S., et al.:
1049 GLODAPv2.2019: An update of GLODAPv2. *Earth System Science Data*, 11(3), 1437-
1050 1461. <https://doi.org/10.5194/essd-11-437-2019>, 2019.
1051
1052 Orr, F. M.: Onshore Geologic Storage of CO₂, *Science*, 25, 325, 1656–1658, doi:
1053 10.1126/science.1175677, 2009.
1054
1055 Otero, P., Ruiz-Villarreal, M., and Peliz, A.: Variability of river plumes off Northwest
1056 Iberia in response to wind events, *Journal of Marine Systems*, 72(1-4), 238–255, 2008.
1057
1058 Padin X. A., Castro, C. G., Ríos, A.F., and Pérez, F.F.: Oceanic CO₂ uptake and
1059 biogeochemical variability during the formation of the Eastern North Atlantic Central
1060 water under two contrasting NAO scenarios, *Journal of Marine Systems*, 84, 3-4, 96–
1061 105, <https://doi.org/10.1016/j.jmarsys.2010.10.002>, 2010.
1062
1063 Pauly, D., and Christensen, V.: Primary production required to sustain global fisheries,
1064 *Nature*, 374(6519), 255–257, 1995.
1065
1066 Pérez, F. F., and Fraga, F.: A precise and rapid analytical procedure for alkalinity
1067 determination, *Marine Chemistry*, 21, 169–182, 1987a.
1068
1069 Pérez, F. F., and Fraga, F.: The pH measurements, in seawater on the NBS scale,
1070 *Marine Chemistry*, 21, 315–327, 1987b.
1071
1072 Pérez, F. F., Rios, A. F., and Rosón, G.: Sea surface carbon dioxide off the Iberian
1073 Peninsula North Eastern Atlantic Ocean, *Journal of Marine Systems*, 19, 27–46, 1999.
1074
1075 Perez, F. F., Alvarez-Salgado, X. A., and Rosón G.: Stoichiometry of the net ecosystem
1076 metabolism in a coastal inlet affected by upwelling. The Ría de H (NW Spain), *Marine*
1077 *Chemistry*, 69, 3-4, 217–236, 2000.
1078
1079 Pérez, F. F., Padin, X. A., Pazos, Y., Gilcoto, M., Cabanas, M., Pardo, P. C., Doval, M.,
1080 D., and Farina-Busto, L.: Plankton response to weakening of the Iberian coastal
1081 upwelling. *Global Change Biology*, 16(4), 1258–1267, 2010.

1082
1083 Pérez, F. F., Velo, A., Padin, X. A., Doval, M. D., Prego, R.: ARIOS DATABASE: An
1084 Acidification Ocean Database for the Galician Upwelling Ecosystem,
1085 Instituto de Investigaciones Marinas, Consejo Superior de Investigaciones Científicas
1086 (CSIC), doi: 10.20350/digitalCSIC/12498, 2020.
1087
1088 Piedracoba, S., Alvarez-Salgado, X. A., Rosón G., and Herrera, J. L.: Short timescale
1089 thermohaline variability and residual circulation in the central segment of the coastal
1090 upwelling system of the Ría de Vigo (northwest Spain) during four contrasting periods,
1091 <https://doi.org/10.1029/2004JC002556>, 2005.
1092
1093 Prego, R., Fraga, F., and Ríos, A. F.: Water interchange between the Ria of Vigo and
1094 the continental shelf. *Scientia Marina* 54, 95–100, 1990.
1095
1096 Raven, J., Caldeira, K., Elderfield, H., Hoegh-Guldberg, O., Liss, P., Riebesell, U.,
1097 Sphepherd, J., Turley, C., and Watson, A.: Ocean acidification due to increasing
1098 atmospheric carbon dioxide: Royal Society Policy Document 12/05, 68 p, 2005.
1099
1100 Ríos, A. F., Pérez, F. F., and Fraga, F.: Water masses in the upper and middle North
1101 Atlantic Ocean east of the Azores, *Deep-Sea Res. Part I*, 39, 645–658, 1992.
1102
1103 Rosón, G., Pérez, F. F., Alvarez-Salgado, X. A., and Figueiras, F. G.: Variation of both
1104 thermohaline and chemical properties in an estuarine upwelling ecosystem -Ría de
1105 Arousa. 1. Time evolution, *Estuarine Coastal and Shelf Science*, 41, 2, 195–213, doi
1106 10.1006/ecss.1995.0061, 1995.
1107
1108 Rosón, G., Cabanas, J. M., Pérez, F. F., Herrera, J. L., Ruiz-Villarreal, M., Castro, C.
1109 G., Piedracoba, S., and Álvarez-Salgado, X. A.: Evidencias do cambio climático na
1110 Hidrografía e a dinámica das Rías e da plataforma galega. Edita: Xunta de Galicia.
1111 Consellería de Medio Ambiente e Desenvolvemento Sostible, *Evidencias e impactos do*
1112 *cambio climático en Galicia*, 287-302, 2009.
1113
1114 Sabine, C. L., Feely, R. A., Gruber, N., Key, R. M., Lee, K., Bullister, J. L.,
1115 Wanninkhof, R., Wong, C. S., Wallace, D. W. R., Tilbrook, B., Millero, F. J., Peng, T.-

1116 H., Kozyr, A., Ono, T., and Rios, A. F.: The oceanic sink for anthropogenic CO₂.
1117 Science 305, 367–371, 2004.
1118
1119 Sarmiento, J. L., and Gruber, N.: Ocean biogeochemical dynamics. Princeton Univ.
1120 Press. 2006.
1121
1122 Souto, C., Gilcoto, M., Fariña-Busto, L., and Pérez, F. F.: Modeling the residual
1123 circulation of a coastal embayment affected by wind-driven upwelling: Circulation of
1124 the Ria de Vigo (NW Spain), Journal of Geophysical Research - Oceans, 108 C11
1125 (3340), doi: 10.1029/2002JC001512, 2003.
1126
1127 SCOR-UNESCO: Determination of Photosynthetic Pigments in Seawater. UNESCO,
1128 Paris, 1966.
1129
1130 Strickland, J. D. H., and Parsons, T.R.: A practical handbook of seawater analysis,
1131 Fisheries Research Board of Canada, Ottawa, Ontario, 1972.
1132
1133 Takeshita, Y., Frieder, C. A., Martz, T. R., Ballard, J. R., Feely, R. A., Kram, S., Nam,
1134 S., Navarro, M. O., Price, N. N., and Smith, J. E.: Including high-frequency variability
1135 in coastal ocean acidification projections, Biogeosciences, 12(19), 5853–5870,
1136 doi:10.5194/bg-12-5853-2015, 2015.
1137
1138 Teira, E., Martínez-García, S., Lonborg, C., and Álvarez-Salgado, X. A.: Growth rates
1139 of different phylogenetic bacterioplankton groups in a coastal upwelling system,
1140 Environmental microbiology reports, 1,6, 545–554, [https://doi.org/10.1111/j.1758-](https://doi.org/10.1111/j.1758-2229.2009.00079.x)
1141 [2229.2009.00079.x](https://doi.org/10.1111/j.1758-2229.2009.00079.x), 2009.
1142
1143 UNESCO: Background papers and supporting data on the Practical Salinity Scale 1978.
1144 UNESCO Tech. Papers in Marine Science, 37, 144pp, 1981.
1145
1146 Uppström, L. R.: Boron = Chlorinity ratio of deep-sea water from Pacific Ocean, Deep-
1147 Sea Res., 21, 161–162, 1974.
1148

1149 Van Heuven, S., Pierrot, D., Rae, J.W.B., Lewis, E., Wallace, D.W.R. MATLAB
1150 Program Developed for CO₂ System Calculations. ORNL/CDIAC-105b. Carbon
1151 Dioxide Information Analysis Center, Oak Ridge National Laboratory, U.S. Department
1152 of Energy, Oak Ridge, Tennessee, 2011.
1153

1154 Velo, A., Pérez, F.F., Lin, X., Key, R.M., Tanhua, T., de la Paz, M., Olsen, A., van
1155 Heuven, S., Jutterström, S., Ríos, A.F.: CARINA data synthesis project: pH data scale
1156 unification and cruise adjustments, *Earth Syst. Sci. Data*, 2, 133–155, doi:10.5194/essd-
1157 2-133-2010, 2010.
1158

1159 Velo, A., Cacabelos, J., Pérez, F.F., Ríos, A.F.: GO-SHIP Software and Manuals:
1160 Software packages and best practice manuals and knowledge transfer for sustained
1161 quality control of hydrographic sections in the Atlantic. (Version v1.0.0), Zenodo,
1162 <http://doi.org/10.5281/zenodo.2603122>, 2019.
1163

1164 Villaceros-Robineau, N., Zúñiga, D., Barreiro-González, B., Alonso-Pérez, F.,
1165 de la Granda, F., and Froján, M.: Bottom boundary layer and particle dynamics in an
1166 upwelling affected continental margin (NW Iberia), *Journal of Geophysical Research:*
1167 *Oceans*, 124, <https://doi.org/10.1029/2019JC015619>, 2019.
1168

1169 Wahl, M., Saderne, V., and Sawall, Y.: How good are we at assessing the impact of
1170 ocean acidification in coastal systems? Limitations, omissions and strengths of
1171 commonly used experimental approaches with special emphasis on the neglected role of
1172 fluctuations, *Mar. Freshw. Res.*, 67, 25–36, doi:10.1071/MF14154, 2016.
1173

1174 Wolf-Gladrow, D. A., Riebesell, U., Burkhardt, S., and Bijma, J.: Direct effects of CO₂
1175 concentration on growth and isotopic composition of marine plankton, *Tellus*, 51B, 461,
1176 1999.
1177

1178 Wooster, W. S., Bakun, A., and McClain, D. R.: The seasonal upwelling cycle along the
1179 eastern boundary of the North Atlantic, *Journal of Marine Research*, 34, 131–141, 1976.
1180

1181 Zúñiga, D., Villaceros-Robineau, N., Salgueiro, E., Alonso-Pérez, F., Rosón, G.,
1182 Abrantes, F., and Castro, C. G.: Particle fluxes in the NW Iberian coastal upwelling

1183 system: Hydrodynamical and biological control. *Continental Shelf Research*, 123
1184 (2016), 89–98, <http://dx.doi.org/10.1016/j.csr.2016.04.008>, 2016.

1185

1186 Zúñiga, D., Santos, C., Froján, M., Salgueiro, E., Rufino, M. M., de la Granda, F.,
1187 Figueiras, F. G., Castro, C. G., and Abrantes, F.: Diatoms as a paleoproductivity proxy
1188 in the NW Iberian coastal upwelling system (NE Atlantic), *Biogeosciences*, 14, 1165–
1189 1179, www.biogeosciences.net/14/1165/2017, 2017.

1190

1191

1192

1193

1194

1195

1196

1197

1198

1199

1200

1201

1202

1203

1204

1205

1206

1207

1208

1209

1210

1211

1212

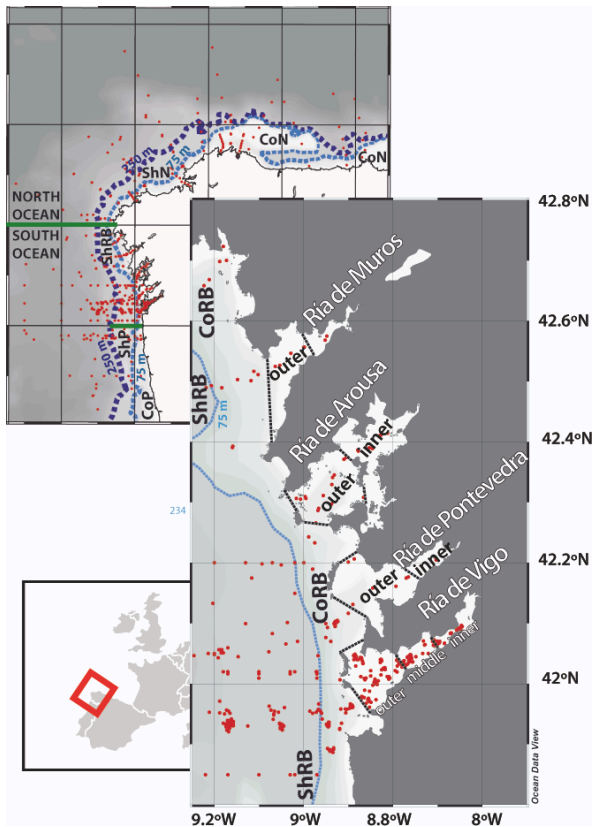
1213

1214

1215

1216

1217



1218

1219

1220 Figure 1. Map of all stations (red dots) including the geographical areas selected to
1221 classify the ARIOS database from isobath of 250 m (dark blue line) and 75 metres (light
1222 blue line), latitudinal criterion (green lines) and geographical lines (black lines).

1223

1224

1225

1226

1227

1228

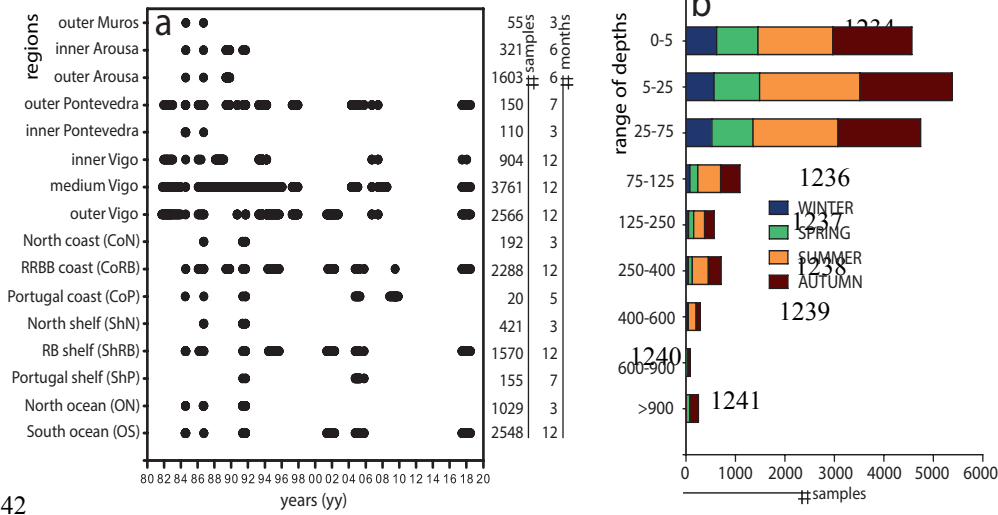
1229

1230

1231

1232

1233



1242

1243 Figure 2. a) Temporal distribution of the observations in the geographical boxes
 1244 included in the ARIOS dataset. b) Seasonal distribution of the measurements in relation
 1245 to depth.

1246

1247

1248

1249

1250

1251

1252

1253

1254

1255

1256

1257

1258

1259

1260

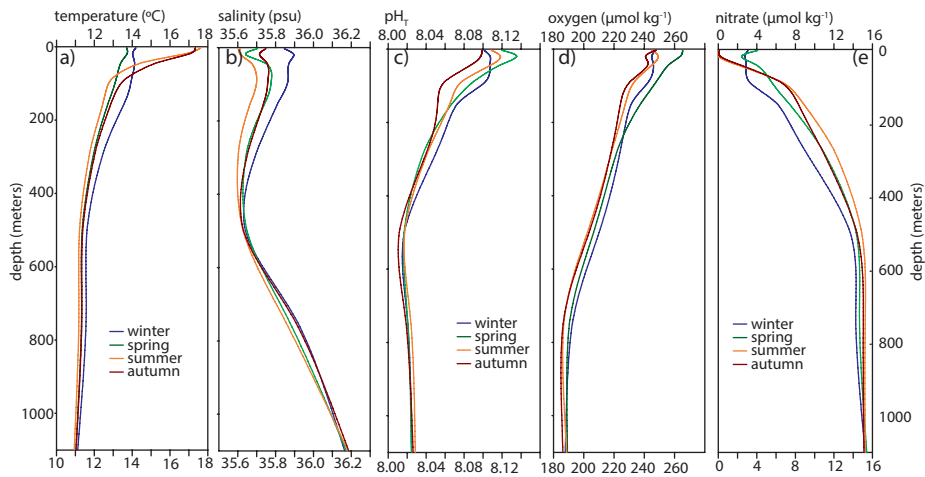
1261

1262

1263

1264

1265



1266

1267

1268 Figure 3. Profiles of seasonal means of temperature (a), salinity (b), pH_T (c), oxygen (d)

1269 and nitrate concentration (e) in the first 1100 meters of the region South Ocean shown

1270 in Fig. 1.

1271

1272

1273

1274

1275

1276

1277

1278

1279

1280

1281

1282

1283

1284

1285

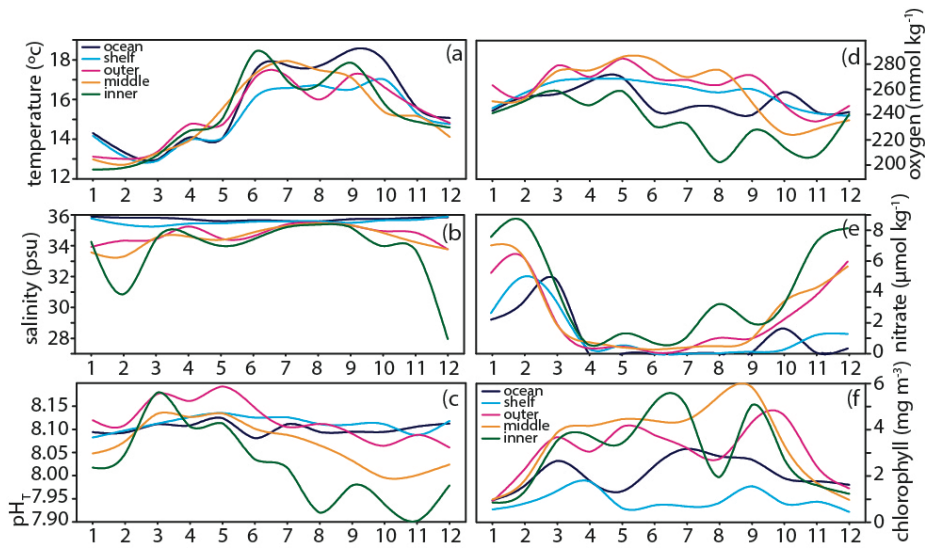
1286

1287

1288

1289

1290



1291

1292

1293 Figure 4. Sea surface (<5 meters depth) seasonal cycles in 1976 - 2018 of temperature
1294 (a), salinity (b), pH_T (c), oxygen concentration (d), nitrate concentration (e) and
1295 chlorophyll (f) at sea surface for five geographical boxes shown in Fig. 1: South Ocean,
1296 RB shelf and outer, middle and inner Ria de Vigo for the entire period of the ARIOS
1297 database.

1298

1299

1300

1301

1302

1303

1304

1305

1306

1307

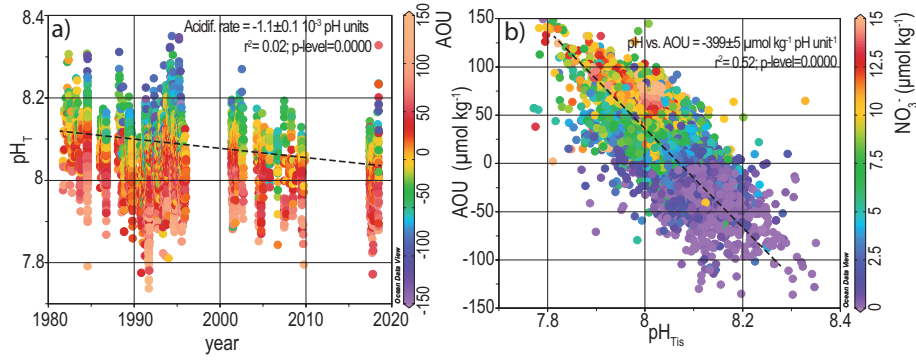
1308

1309

1310

1311

1312



1313

1314 Figure 5. Time-series of pH ARIOS data. The black line depicts the long-term trend.

1315 Scatter diagram of AOU vs pH_T including the nitrate concentration shown as colour of
1316 every dot.

1317

1318

1319

1320

1321

1322

1323

1324

1325

1326

1327

1328

1329

1330

1331

1332

1333

1334

1335

1336

1337

1338 Table 1. Discrete measurements of projects gathered in the ARIOS database and
1339 associated information: including dates, the number of days between the start and the
1340 end of sampling period (#d), sample number (#), the principal investigator (PI),
1341 measured parameters, link to data repository and the sampled geographical area.

1342

1343 - All projects include measurements of *T*, *S*. Others as *pH*, alkalinity (*Alk*), nutrient
1344 (*Nut*), oxygen (*O₂*) concentration, chlorophyll (*Chla*) are indicated.

1345 - The concentration units of these variables are $\mu\text{mol kg}^{-1}$ or $\mu\text{mol L}^{-1}$ (*) and the *pH*
1346 measurements in NBS scale (°) or in total scale.

1347 - Regions are identified as ocean (*O*), shelf (*Sh*), coastal (*Co*), Ría de Vigo (*RV*), Ría de
1348 Pontevedra (*RP*), Ría de Arousa (*RA*) and Ría de Muros (*RM*) while the superscript
1349 index means south (^{*S*}), north (^{*N*}), Portugal (^{*P*}), Rías Baixas (^{*RB*}), outer (^{*O*}), middle (^{*M*})
1350 and inner (^{*I*}).

1351

1352

1353

1354

1355

1356

1357

1358

1359

1360

1361

1362

1363

1364

1365

1366

1367

1368

1369

1370

1371

1372

1373

	SS_{range}	r^2_{ss}	$t_{\text{interannual}}$	r^2	p-value
OCEAN	0.050	0.17	-0.0012±0.0002	0.21	0.0000
SHELF	0.050	0.06	-0.0017±0.0003	0.15	0.0009
OUTER	0.120	0.24	-0.0027±0.0003	0.21	0.0000
MIDDLE	0.130	0.28	-0.0022±0.0005	0.03	0.0000
INNER	0.260	0.47	-0.0039±0.0005	0.34	0.0000

1374

1375 Table 2: Seasonal amplitude of monthly pH means (SS_{range}) and long-term trends
1376 ($t_{\text{interannual}}$) of pH in five regions and significant regression coefficients between the in
1377 situ pH measurements and the monthly mean pH values (r^2_{ss}) and the regression
1378 coefficient of the temporal variability of the deseasonalized pH measurements (r^2).

1379

1380

1381

1382

1383

1384

1385

1386

1387

1388

1389

1390

1391

1392

1393

1394

1395

1396

1397

1398

1399

1400

1401 Appendix A

1402

1403 Table A1: Vertical distribution of seasonal mean values and standard deviation (mean \pm
1404 standard deviation) of temperature, salinity, pH_T, oxygen and nitrate in the region South
1405 Ocean shown in Fig. 1.

z (m)	winter	spring	summer	autumn
temperature (°C)				
0-5	13.6±0.5	13.4±0.7	17.9±0.7	17.7±1.5
5-25	13.8±0.7	13.6±0.6	17.1±0.7	17.2±1.5
25-75	13.9±0.6	13.2±0.4	14.1±0.5	14.9±1.0
75-125	13.7±0.6	13.0±0.5	12.8±0.3	13.2±0.4
125-200	13.5±0.6	12.6±0.4	12.3±0.3	12.6±0.3
200-400	12.6±0.3	11.9±0.3	11.6±0.3	11.9±0.3
400-600	11.5±0.1	11.3±0.1	11.1±0.2	11.2±0.2
600-900			11.4±0.1	11.4±0.2
900-1300	11.2±0.1	11.1±0.2	10.9±0.3	11.0±0.3
salinity				
0-5	35.82±0.06	35.72±0.11	35.62±0.07	35.71±0.08
5-25	35.85±0.06	35.67±0.15	35.62±0.07	35.69±0.09
25-75	35.85±0.05	35.74±0.09	35.71±0.06	35.76±0.08
75-125	35.86±0.07	35.76±0.07	35.70±0.04	35.76±0.07
125-200	35.80±0.10	35.73±0.06	35.64±0.04	35.72±0.06
200-400	35.71±0.04	35.65±0.04	35.59±0.05	35.64±0.05
400-600	35.64±0.04	35.65±0.05	35.64±0.05	35.64±0.03
600-900			35.89±0.09	35.99±0.06
900-1300	36.17±0.02	36.18±0.02	36.19±0.03	36.17±0.07
pH_T				
0-5	8.10±0.02	8.12±0.02	8.11±0.02	8.09±0.02
5-25	8.11±0.02	8.14±0.02	8.12±0.02	8.09±0.02
25-75	8.11±0.01	8.12±0.01	8.11±0.02	8.08±0.02
75-125	8.10±0.01	8.09±0.02	8.08±0.03	8.06±0.02
125-200	8.07±0.03	8.07±0.03	8.06±0.03	8.05±0.02
200-400	8.05±0.01	8.04±0.01	8.04±0.02	8.03±0.01
400-600	8.02±0.01	8.017±0.002	8.02±0.02	8.01±0.01
600-900			8.01±0.02	7.984±0.003
900-1300	8.025±0.004	8.024±0.002	8.03±0.01	8.01±0.02
oxygen (μmol kg⁻¹)				
0-5	249±6	265±17	250±12	244±12
5-25	250±7	267±13	253±10	240±7
25-75	249±8	255±9	247±7	236±8
75-125	247±9	247±9	232±4	227±7
125-200	230±11	237±9	226±6	224±6
200-400	227±11	224±8	213±7	220±8
400-600	209±6	205±5	196±7	200±4
600-900			186±2	184±2
900-1300	187±1	189±3	188±4	185±3

1406

1407

1408

1409

1410

1411

1412

TONI PADIN 5/8/2020 11:44

Eliminado: _

TONI PADIN 31/7/2020 15:12

Con formato: Subíndice

1414

1415 | Table A2: Monthly mean values and standard deviation (mean ± standard deviation) of
 1416 temperature, salinity, pH_T, oxygen concentration, nitrate concentration and chlorophyll
 1417 at the surface waters for five geographical boxes shown in Fig. 1: South Ocean, RB
 1418 shelf and outer, middle and inner Ría de Vigo.

TONI PADIN 5/8/2020 11:44
 Con formato: Fuente: Sin Negrita
 TONI PADIN 5/8/2020 11:44
 Eliminado:

	month	OCEAN	SHELF	OUTER	MIDDLE	INNER
temperature (°C)	Jan	14.3±0.4	14.2±0.4	13.1±0.8	13.0±0.7	12.5±0.4
	Feb	13.3±0.2	13.1±0.6	13.0±0.7	12.7±0.7	12.6±0.7
	Mar	13.0±0.6	12.9±0.5	13.4±0.4	13.3±0.6	13.2±0.6
	Apr	14.1±0.4	14.0±0.3	14.8±1.2	14.0±0.9	14.4±1.1
	May	14.1±0.9	14.1±1.1	14.7±1.0	15.6±1.5	15.1±1.3
	Jun	17.5±1.1	16.1±0.9	17.1±1.0	17.3±1.3	18.4±1.1
	Jul	17.7±0.6	16.6±1.0	17.2±1.0	17.9±1.5	16.9±1.2
	Aug	17.7±0.9	16.7±0.6	16.0±1.7	17.5±1.5	16.8±1.7
	Sep	18.5±1.3	16.5±1.3	17.3±1.3	17.1±1.2	17.8±1.4
	Oct	17.9±0.4	17.0±0.6	16.6±0.9	15.4±1.1	15.8±1.0
	Nov	15.6±0.6	15.3±1.1	15.6±1.4	15.2±0.9	14.9±1.2
	Dec	15.1±0.3	14.8±0.2	14.8±1.3	14.1±0.9	14.6±1.1
salinity	Jan	35.88±0.13	35.77±0.18	33.92±0.82	33.57±2.37	34.26±1.44
	Feb	35.81±0.04	35.37±0.84	34.33±1.63	33.30±2.51	30.86±4.78
	Mar	35.81±0.04	35.24±0.71	34.43±0.77	34.52±1.12	34.42±1.25
	Apr	35.72±0.07	35.43±0.47	35.24±0.29	34.58±0.90	34.72±0.74
	May	35.59±0.12	35.45±0.25	34.47±1.37	34.38±1.09	33.99±2.29
	Jun	35.64±0.13	35.56±0.12	34.62±0.81	34.87±0.74	34.42±0.54
	Jul	35.60±0.07	35.58±0.08	35.36±0.26	35.27±0.38	35.19±0.50
	Aug	35.57±0.05	35.59±0.05	35.48±0.22	35.45±0.21	35.37±0.17
	Sep	35.72±0.12	35.48±0.18	35.33±0.19	35.32±0.29	35.20±0.27
	Oct	35.74±0.05	35.65±0.10	34.94±0.56	34.84±0.88	33.98±1.45
	Nov	35.81±0.06	35.67±0.11	34.85±0.77	34.23±0.85	33.73±2.80
	Dec	35.85±0.06	35.89±0.26	33.76±1.36	33.77±1.51	27.95±5.50
pH _T	Jan	8.09±0.03	8.08±0.03	8.12±0.06	8.05±0.05	8.02±0.04
	Feb	8.09±0.02	8.10±0.03	8.11±0.05	8.07±0.05	8.05±0.06
	Mar	8.11±0.01	8.11±0.03	8.18±0.08	8.13±0.07	8.18±0.08
	Apr	8.11±0.02	8.13±0.03	8.16±0.05	8.13±0.05	8.11±0.07
	May	8.12±0.02	8.14±0.04	8.19±0.04	8.13±0.08	8.11±0.07
	Jun	8.08±0.03	8.13±0.03	8.15±0.04	8.10±0.07	8.04±0.09
	Jul	8.11±0.02	8.13±0.02	8.11±0.06	8.09±0.07	8.02±0.07
	Aug	8.09±0.03	8.11±0.03	8.11±0.07	8.07±0.09	7.92±0.05
	Sep	8.09±0.02	8.11±0.03	8.09±0.05	8.03±0.07	7.98±0.11
	Oct	8.09±0.01	8.11±0.03	8.06±0.06	8.00±0.08	7.94±0.09
	Nov	8.11±0.02	8.09±0.02	8.09±0.07	8.00±0.06	7.90±0.12
	Dec	8.11±0.01	8.12±0.01	8.06±0.03	8.02±0.04	7.98±0.02

1419

1421
1422
1423
1424
1425
1426

Table A2; Continued

	month	OCEAN	SHELF	OUTER	MIDDLE	INNER
oxygen ($\mu\text{mol kg}^{-1}$)	Jan	244±6	246±5	265±8	252±16	242±11
	Feb	255±5	259±12	255±13	254±15	252±14
	Mar	258±16	268±19	280±27	276±23	260±28
	Apr	268±5	270±7	271±13	276±25	249±26
	May	271±13	269±14	286±22	287±25	260±12
	Jun	244±3	266±11	270±17	284±26	232±19
	Jul	247±12	263±11	269±23	271±25	234±23
	Aug	247±9	259±8	265±23	277±27	204±21
	Sep	241±9	261±14	272±18	251±26	228±34
	Oct	259±13	250±12	249±20	226±21	215±16
	Nov	243±11	242±4	236±9	230±16	209±26
	Dec	243±10	240±12	248±11	237±14	242±16
nitrate ($\mu\text{mol kg}^{-1}$)	Jan	2.3±0.5	2.7±0.8	5.3±2.6	7.1±3.8	7.6±2.0
	Feb	3.4±0.7	5.0±2.6	6.3±3.0	6.3±3.4	8.6±4.5
	Mar	4.9±2.4	3.5±2.9	2.1±2.5	2.0±2.4	4.5±2.3
	Apr	0.1±2.4	0.4±0.7	0.4±0.5	0.8±1.0	0.6±0.6
	May	0.02±0.03	0.6±0.4	0.5±0.4	0.5±0.8	0.7±1.3
	Jun	0.04±0.02	0.1±0.1	0.1±0.3	0.3±0.4	0.8±0.8
	Jul	0.1±0.1	0.0±0.1	0.3±0.6	0.5±0.7	1.1±0.8
	Aug	0.08±0.03	0.1±0.1	1.1±1.6	0.6±0.9	3.3±3.2
	Sep	0.1±0.1	0.2±0.7	1.0±0.9	0.9±1.1	2.1±1.4
	Oct	1.7±0.8	0.3±0.7	2.2±2.4	3.4±2.7	3.1±1.5
	Nov	0.1±0.1	1.2±2.9	3.8±2.9	4.3±2.3	7.2±3.2
	Dec	0.4±0.9	1.3±1.0	6.0±3.1	5.7±2.7	8.2±4.1
chlorophyll (mg m^{-3})	Jan	0.5±0.1	0.6±0.1	0.9±0.2	1.0±0.9	0.9±0.3
	Feb	0.5±0.1	0.8±0.3	2.3±1.5	1.8±1.6	1.3±0.9
	Mar	0.5±0.2	1.4±1.5	3.7±2.8	3.9±3.2	3.5±2.3
	Apr	2.6±1.1	1.8±1.4	3.0±1.8	4.2±2.4	3.7±2.1
	May	0.5±0.2	0.6±0.6	4.1±3.0	4.5±4.5	3.4±2.6
	Jun	0.8±0.8	0.7±0.6	3.8±1.7	4.4±2.7	5.2±3.2
	Jul	0.4±0.2	0.7±0.7	3.2±1.9	4.4±2.5	5.0±2.2
	Aug	0.5±0.2	0.8±0.5	2.7±2.3	5.5±4.1	2.0±2.3
	Sep	0.5±0.3	1.6±1.0	4.3±2.4	5.8±3.6	5.1±3.7
	Oct	0.3±0.1	0.8±0.5	4.6±4.1	3.3±3.5	2.7±1.9
	Nov	0.8±0.3	0.9±0.8	2.4±1.1	1.7±2.4	1.6±1.0
	Dec	0.5±0.2	0.4±0.6	1.5±0.8	1.0±0.6	1.2±0.3

1427
1428
1429
1430
1431

TONI PADIN 5/8/2020 11:44

Con formato: Fuente: Sin Negrita

TONI PADIN 5/8/2020 11:44

Eliminado: